

CONFIDENTIAL

Copy 327
RM L55A21a



CASE FILE
COPY

RESEARCH MEMORANDUM

STATIC LATERAL STABILITY DATA FROM AN EXPLORATORY
INVESTIGATION AT A MACH NUMBER OF 6.86 OF AN
AIRPLANE CONFIGURATION HAVING A WING
OF TRAPEZOIDAL PLAN FORM

By Herbert W. Ridyard, David E. Fetterman, Jr.,
and Jim A. Penland

Langley Aeronautical Laboratory
Langley Field, Va.

CLASSIFICATION CHANGED TO UNCLASSIFIED

AUTHORITY: NASA TECHNICAL PUBLICATIONS
ANNOUNCEMENTS NO. 55

EFFECTIVE DATE: SEPTEMBER 1, 1961

CLASSIFIED DOCUMENT

This material contains information affecting the National Defense of the United States within the meaning of the espionage laws, Title 18, U.S.C., Secs. 793 and 794, the transmission or revelation of which in any manner to an unauthorized person is prohibited by law.

NATIONAL ADVISORY COMMITTEE FOR AERONAUTICS

WASHINGTON

February 15, 1955

CONFIDENTIAL

NATIONAL ADVISORY COMMITTEE FOR AERONAUTICS

RESEARCH MEMORANDUM

STATIC LATERAL STABILITY DATA FROM AN EXPLORATORY
INVESTIGATION AT A MACH NUMBER OF 6.86 OF AN
AIRPLANE CONFIGURATION HAVING A WING
OF TRAPEZOIDAL PLAN FORM

By Herbert W. Ridyard, David E. Fetterman, Jr.,
and Jim A. Penland

SUMMARY

An investigation to determine the static lateral stability characteristics of an airplane configuration having a trapezoidal wing with modified hexagonal airfoil section and tail surfaces with 5° semiangle wedge sections has been carried out in the Langley 11-inch hypersonic tunnel. The tests were made at a Mach number of 6.86 and a Reynolds number of 343,000 based on wing mean aerodynamic chord. Data were obtained for angles of sideslip up to 10° and angles of attack up to 25° for the complete model and various combinations of its components. The data are presented with respect to the body axes.

INTRODUCTION

The aircraft configurations previously investigated experimentally at hypersonic speeds have been restricted mainly to missile types which were not required to be able to land and which, therefore, had relatively small wings or wings of low aspect ratio. The purpose of the present investigation was to determine the characteristics of a configuration conforming more closely to a piloted aircraft having a wing area sufficient for conventional landing. Of the various possible configurations, one was selected for this exploratory study which was expected to have satisfactory low-speed characteristics and satisfactory transonic characteristics. This configuration (fig. 1) employs a trapezoidal wing and the arrangement, in general, is similar to conventional airplanes. Two particular features were incorporated which are believed to be desirable for hypersonic operation - relatively large leading-edge radii for both wing and tail and wedge-shaped sections for the tail surfaces. The large

leading-edge radius is essential in order to keep the heat-transfer rates within feasible limits, and the wedge tail sections were selected to provide the desired tail effectiveness with tail surfaces of conventional size (ref. 1).

Six-component data have been obtained both for the complete model and for various components. The lift, drag, and static longitudinal stability data of the model and its components at $M = 6.86$ are presented in reference 2 and both static longitudinal and lateral stability data at a Mach number of 4.06 may be found in reference 3. The present paper contains the static lateral stability results, that is, the variations of the aerodynamic coefficients with sideslip angle, at $M = 6.86$. Detailed analysis of the stability parameters is omitted in order to expedite release of this information.

COEFFICIENTS AND SYMBOLS

The results of the tests are presented as standard NACA coefficients of forces and moments. The data are referred to the body-axes system but may be converted to the stability-axes system by means of the conversion equations given in the appendix. The body- and stability-axes systems are illustrated in figure 2. The moment reference is at 54 percent of the wing mean aerodynamic chord or at 52.66 percent of the body length measured from the nose. The coefficients and symbols are defined as follows:

C_N	normal-force coefficient, $-Z/qS$
C_Y	lateral-force coefficient, Y/qS
C_l	rolling-moment coefficient, L/qSb
C_m	pitching-moment coefficient, $M'/qS\bar{c}$
C_n	yawing-moment coefficient, N/qSb
Z	force along Z-axis, lb
Y	force along Y-axis, lb
L	moment about X-axis, in-lb
M'	moment about Y-axis, in-lb

N	moment about Z-axis, in-lb
q	free-stream dynamic pressure, lb/sq in.
S	total wing area including body intercept, sq in.
b	wing span, in.
c	wing chord, in.
\bar{c}	wing mean aerodynamic chord, in.
c_t	tail chord, in.
M	Mach number
R	Reynolds number
α	angle of attack, deg
β	angle of sideslip, deg

$$C_{Y\beta} = \left(\frac{\partial C_Y}{\partial \beta} \right)_{\beta=0}$$

$$C_{Z\beta} = \left(\frac{\partial C_Z}{\partial \beta} \right)_{\beta=0}$$

$$C_{n\beta} = \left(\frac{\partial C_n}{\partial \beta} \right)_{\beta=0}$$

Subscripts:

B	body-axes system
S	stability-axes system

MODELS AND APPARATUS

Models

The model configurations used for the present tests consisted of a complete model (fig. 1), a body alone, a body-wing combination, and a body-tail combination. Details concerning the airplane model are given in the three-view drawing (fig. 3), in the sketches of the airfoil sections (fig. 4), and in the table of geometric characteristics (table I). The complete model mounted for testing in the tunnel is shown in figure 5. A discussion of some of the design features of the model is included in reference 2.

Balance and Model Support

The strain-gage balance used for the present tests was initially designed to measure only four components - normal force, pitching moment, yawing moment, and lateral force. In order to adapt the balance for use in the present program, strain gages were added to the balance sting and calibrated to measure rolling moment. This method of obtaining a rolling-moment component resulted in less sensitivity than desired. This resulting sacrifice in accuracy was considered more than compensated for by the saving of the time necessary for the design, construction, and calibration of a new five-component balance.

The model was attached to the balance so that constant geometry between model and balance was maintained for all test angles. The model was placed at an angle of sideslip by means of a bent sting; angles of attack were obtained by rotating the model and balance about a horizontal axis normal to the wind stream. This type of model rotation necessitated calculation of corrected angles of attack and sideslip. Model deflections due to aerodynamic loads were incorporated in these corrected test angles. These model deflections were obtained through the use of angles measured from schlieren photographs and the balance calibration.

Wind Tunnel

The tests were conducted in the Langley 11-inch hypersonic tunnel. For this investigation the tunnel was equipped with a single-step two-dimensional nozzle constructed of Invar. The nozzle is designed by the method of characteristics with a correction made for boundary layer and operates at an average Mach number of 6.86. The duration of each run was about 80 seconds, and the variation of test section Mach number with time is negligible after the first 15 seconds of running time. This constant Mach number flow made it possible to obtain forces for several

angles of attack during each run. The model was held at low angles of attack for starting and stopping the runs in order to minimize shock loads on the strain-gage balance which supports the model.

Tests

Tests were made at an average stagnation temperature of 675° F to avoid air liquefaction (ref. 4), a stagnation pressure of 20 atmospheres absolute, and a test Mach number of 6.86. These conditions correspond to a Reynolds number of 343,000 based on wing mean aerodynamic chord. The absolute humidity was kept to less than 1.87×10^{-5} pounds of water per pound of dry air for all tests. Tests were made at angles of sideslip β from -5° to 10° for an angle of attack of 0° and from $\beta = 0^\circ$ to about 10° for angles of attack up to 25°.

PRECISION OF DATA

The probable uncertainties in the force and moment coefficients for individual test points - due to the balance system, and variations in the dynamic pressure - have been evaluated and are presented as follows:

C_N	± 0.02
C_m	± 0.005
C_Y	± 0.005
C_n	± 0.0015
C_l	± 0.003

In general, the faired curves should be more accurate than these values.

The angle of attack α and angle of sideslip β were accurate within $\pm 0.10^\circ$.

SUMMARY OF RESULTS

The experimental aerodynamic characteristics of the models are tabulated for each combination of corrected angle of attack and sideslip in table II. The data are presented with respect to the body-axes system.

The variations with sideslip angle of the aerodynamic characteristics, C_Y , C_n , C_l , C_N , and C_m , for various angles of attack for the complete model and for other combinations of the component parts are given

in figures 6 to 10. The curves presented in these figures are for nominal angles of attack and were obtained by fairing data taken from table II. In general, the variations of the coefficients C_Y and C_N with β presented in figures 6 and 7 are linear at low angles of attack. At high angles of attack the variations of the coefficients with β show some nonlinearities. The variations of C_L , C_N , and C_m with β in figures 8 to 10 are small and for most cases are linear. Some irregularities in these curves are present; for example, the variation of C_N with β for the complete model (fig. 9(a)). These irregularities may possibly be attributed to difficulties in fairing data with considerable scatter.

In figure 11 typical schlieren photographs are shown of the complete model and body-wing configuration at various angles of sideslip.

The variation of the slope parameters $C_{Y\beta}$, $C_{N\beta}$, and $C_{L\beta}$ with α for the complete model and other model configurations is presented in figures 12 to 14. Attention is called to the small but positive values of $C_{L\beta}$ (negative effective dihedral) exhibited by the complete model at positive angles of attack. (See fig. 14.)

Langley Aeronautical Laboratory,
National Advisory Committee for Aeronautics,
Langley Field, Va., January 4, 1955.

APPENDIX

AXES-TRANSFER EQUATIONS

The equations for transfer of force and moment coefficients from the body-axes system to the stability-axes system are as follows:

$$C_{Y_S} = C_{Y_B}$$

$$C_{l_S} = C_{l_B} \cos \alpha + C_{n_B} \sin \alpha$$

$$C_{n_S} = C_{n_B} \cos \alpha - C_{l_B} \sin \alpha$$

$$C_{m_S} = C_{m_B}$$

Inasmuch as the longitudinal or axial force was only measured for $\beta = 0$, the axes transfer equations for lift and drag coefficients are not given here. Lift and drag coefficients for $\beta = 0$ are presented in reference 2.

REFERENCES

1. McLellan, Charles H.: A Method for Increasing the Effectiveness of Stabilizing Surfaces at High Supersonic Mach Numbers. NACA RM L54F21, 1954.
2. Penland, Jim A., Ridyard, Herbert W., and Fetterman, David E., Jr.: Lift, Drag, and Static Longitudinal Stability Data From an Exploratory Investigation at a Mach Number of 6.86 of an Airplane Configuration Having a Wing of Trapezoidal Plan Form. NACA RM L54L03b, 1955.
3. Dunning, Robert W., and Ulmann, Edward F.: Static Longitudinal and Lateral Stability Data From an Exploratory Investigation at Mach Number 4.06 of an Airplane Configuration Having a Wing of Trapezoidal Plan Form. NACA RM L55A21, 1955.
4. McLellan, Charles H., and Williams, Thomas W.: Liquefaction of Air in the Langley 11-Inch Hypersonic Tunnel. NACA TN 3302, 1954.

TABLE I.- GEOMETRIC CHARACTERISTICS OF MODEL

Wing:

Area (including area submerged in fuselage), sq in.	6.24
Span, in.	4.33
Mean aerodynamic chord, in.	1.716
Root chord, in.	2.53
Tip chord, in.	0.354
Airfoil section	Hexagonal with round leading edge
Taper ratio	0.140
Aspect ratio	3.00
Sweep of leading edge, deg	38.83
Sweep of quarter-chord line, deg	29
Incidence at fuselage center line, deg	0
Dihedral, deg	0
Geometric twist, deg	0

Horizontal or vertical tails:

Area (including area submerged in fuselage), sq in.	2.06
Span, in.	2.69
Mean aerodynamic chord, in.	0.853
Root chord, in.	1.214
Tip chord, in.	0.317
Airfoil section	5° semiangle wedge
Taper ratio	0.261
Aspect ratio	3.52
Sweep of leading edge, deg	22.63
Dihedral, deg	0

Fuselage:

Length, in.	7.50
Maximum diameter, in.	0.790
Fineness ratio	9.50
Base diameter, in.	0.790
Distance from nose to moment reference	3.950
Ogive nose length, in.	2.29
Ogive radius, in.	6.85

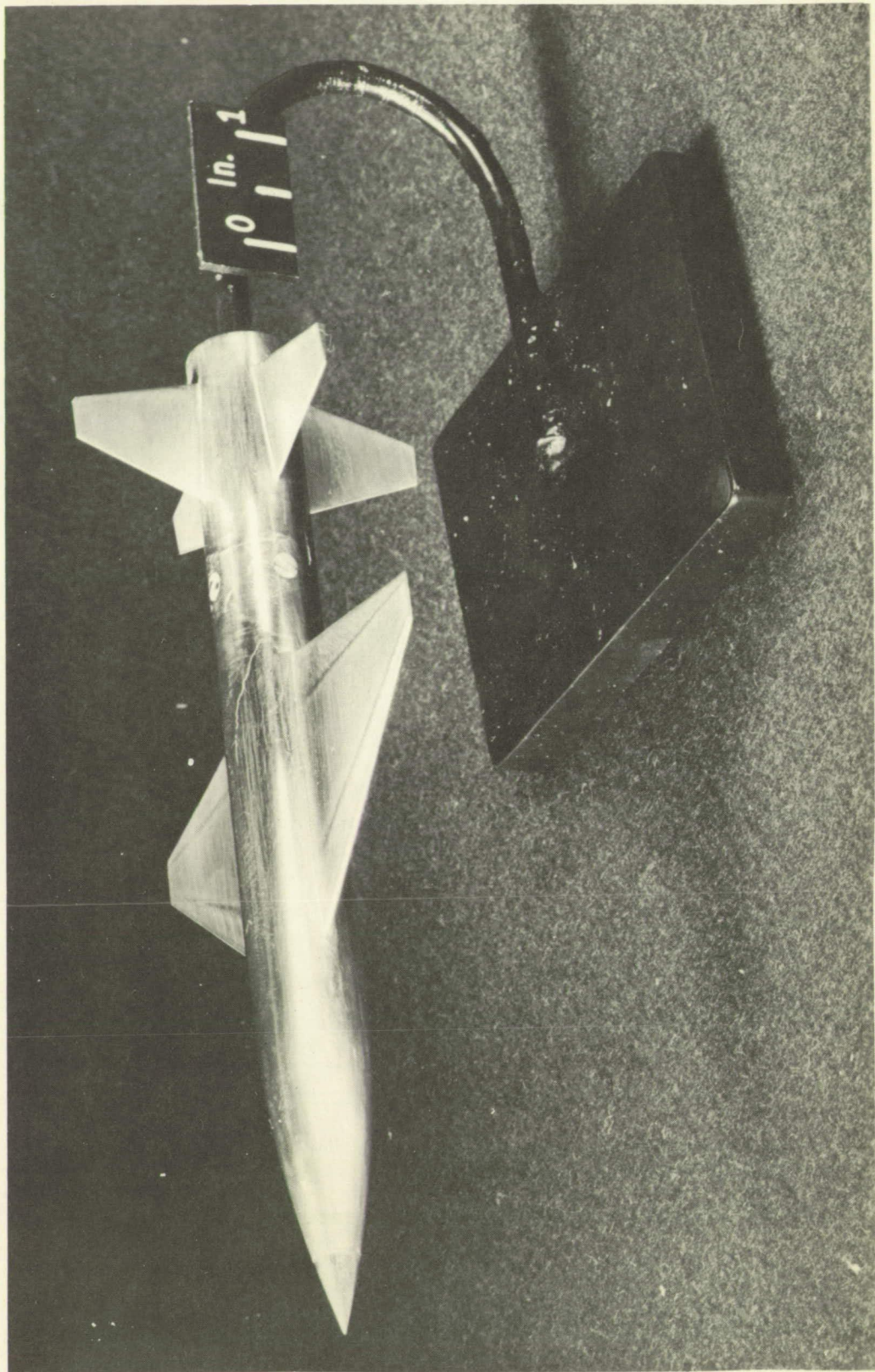
TABLE II.- AERODYNAMIC CHARACTERISTICS OF THE MODEL AND VARIOUS COMBINATIONS OF ITS COMPONENTS AT M = 6.86; R = 343,000 - Concluded

[Body-axis data]

(d) Body-alone configuration

α , deg	β , deg	C_N	C_m	C_l	C_n	C_Y
.00	-.17	.0027	.0000	.0008	.0001	.0004
.00	-.07	-.0033	.0006	.0002	.0001	.0005
.00	.88	.0003	-.0001	.0017	-.0021	-.0018
.00	.93	-.0002	-.0007	-.0013	-.0019	-.0019
.00	1.80	.0040	-.0002	.0012	-.0034	-.0065
.00	1.82	.0033	-.0001	-.0006	-.0034	-.0062
.00	2.72	.0027	-.0002	.0010	-.0046	-.0118
.00	2.82	-.0001	-.0006	-.0007	-.0045	-.0108
.00	3.77	.0027	-.0001	.0007	-.0057	-.0164
.00	3.82	.0032	-.0007	-.0012	-.0056	-.0169
.00	4.82	.0032	-.0000	-.0014	-.0065	-.0221
.00	4.82	.0014	-.0001	.0005	-.0068	-.0227
.00	5.72	.0028	-.0002	.0011	-.0078	-.0290
.00	5.87	.0048	-.0004	-.0018	-.0075	-.0282
.00	7.68	.0030	-.0006	-.0024	-.0097	-.0420
.00	7.92	.0027	-.0003	.0004	-.0097	-.0433
.00	9.75	.0046	-.0003	-.0032	-.0113	-.0573
.00	10.00	.0026	-.0004	-.0002	-.0115	-.0575
.02	.00	-.0002	.0008	-.0009	-.0000	-.0001
1.05	.00	.0038	.0057	-.0004	-.0000	-.0001
1.93	.00	.0167	.0091	-.0004	.0003	-.0010
2.95	.00	.0179	.0124	-.0006	.0002	-.0000
4.00	.00	.0179	.0149	-.0006	.0001	.0003
5.02	.00	.0245	.0174	-.0002	.0002	-.0004
5.98	.00	.0374	.0198	-.0010	.0002	-.0004
7.97	.00	.0490	.0247	-.0009	.0003	.0004
9.97	.00	.0631	.0289	-.0019	.0004	.0000
11.90	.00	.0839	.0322	-.0023	.0004	-.0004
13.93	.00	.0999	.0349	-.0006	.0004	-.0001
16.00	.00	.1135	.0378	.0012	-.0002	-.0008
17.98	.00	.1382	.0389	.0007	-.0003	-.0000
20.03	.00	.1685	.0391	.0007	-.0002	-.0018
21.93	.00	.2003	.0393	.0008	-.0001	-.0007
23.95	.00	.2288	.0395	.0020	-.0001	-.0011
25.90	.00	.2621	.0397	.0010	-.0001	-.0011

α , deg	β , deg	C_N	C_m	C_l	C_n	C_Y
.25	5.10	.0012	.0008	-.0005	-.0065	-.0250
1.23	5.10	.0050	.0041	-.0009	-.0065	-.0256
2.26	5.10	.0089	.0076	-.0012	-.0066	-.0259
3.26	5.09	.0117	.0108	-.0006	-.0064	-.0274
4.20	5.09	.0157	.0138	-.0009	-.0063	-.0281
5.20	5.09	.0276	.0170	-.0018	-.0061	-.0285
6.27	5.09	.0303	.0197	-.0020	-.0059	-.0287
8.28	5.08	.0526	.0246	-.0016	-.0054	-.0301
10.27	5.08	.0682	.0288	.0000	-.0051	-.0322
12.22	5.07	.0850	.0320	-.0011	-.0044	-.0342
14.28	5.07	.1062	.0347	.0003	-.0042	-.0357
16.29	5.08	.1275	.0365	.0006	-.0046	-.0377
18.37	5.07	.1524	.0376	.0009	-.0040	-.0398
20.32	5.07	.1799	.0380	.0011	-.0036	-.0416
20.31	5.07	.2088	.0382	.0011	-.0033	-.0432
24.31	5.06	.2385	.0381	.0002	-.0030	-.0443
26.31	5.06	.2753	.0384	.0017	-.0027	-.0476
.48	10.17	.0026	.0041	.0005	-.0106	-.0585
1.50	10.17	.0028	.0049	.0014	-.0107	-.0597
1.88	10.17	.0066	.0066	.0011	-.0107	-.0601
3.40	10.17	.0142	.0096	.0005	-.0106	-.0602
4.45	10.17	.0219	.0118	.0009	-.0103	-.0608
5.50	10.16	.0262	.0145	.0024	-.0103	-.0622
6.58	10.16	.0379	.0169	.0016	-.0102	-.0643
8.60	10.16	.0549	.0209	.0023	-.0097	-.0658
10.63	10.15	.0604	.0244	.0037	-.0091	-.0684
12.53	10.14	.0914	.0273	.0035	-.0083	-.0720
14.68	10.14	.1171	.0290	.0027	-.0074	-.0760
16.71	10.14	.1435	.0314	-.0002	-.0071	-.0810
18.68	10.13	.1710	.0324	.0008	-.0064	-.0864
20.71	10.13	.1972	.0332	.0001	-.0060	-.0887
22.73	10.12	.2283	.0335	.0009	-.0054	-.0927
24.66	10.12	.2617	.0336	.0007	-.0050	-.0959
26.73	10.11	.2950	.0336	.0006	-.0045	-.0985



L-86687

Figure 1.- Photograph of complete-model configuration.

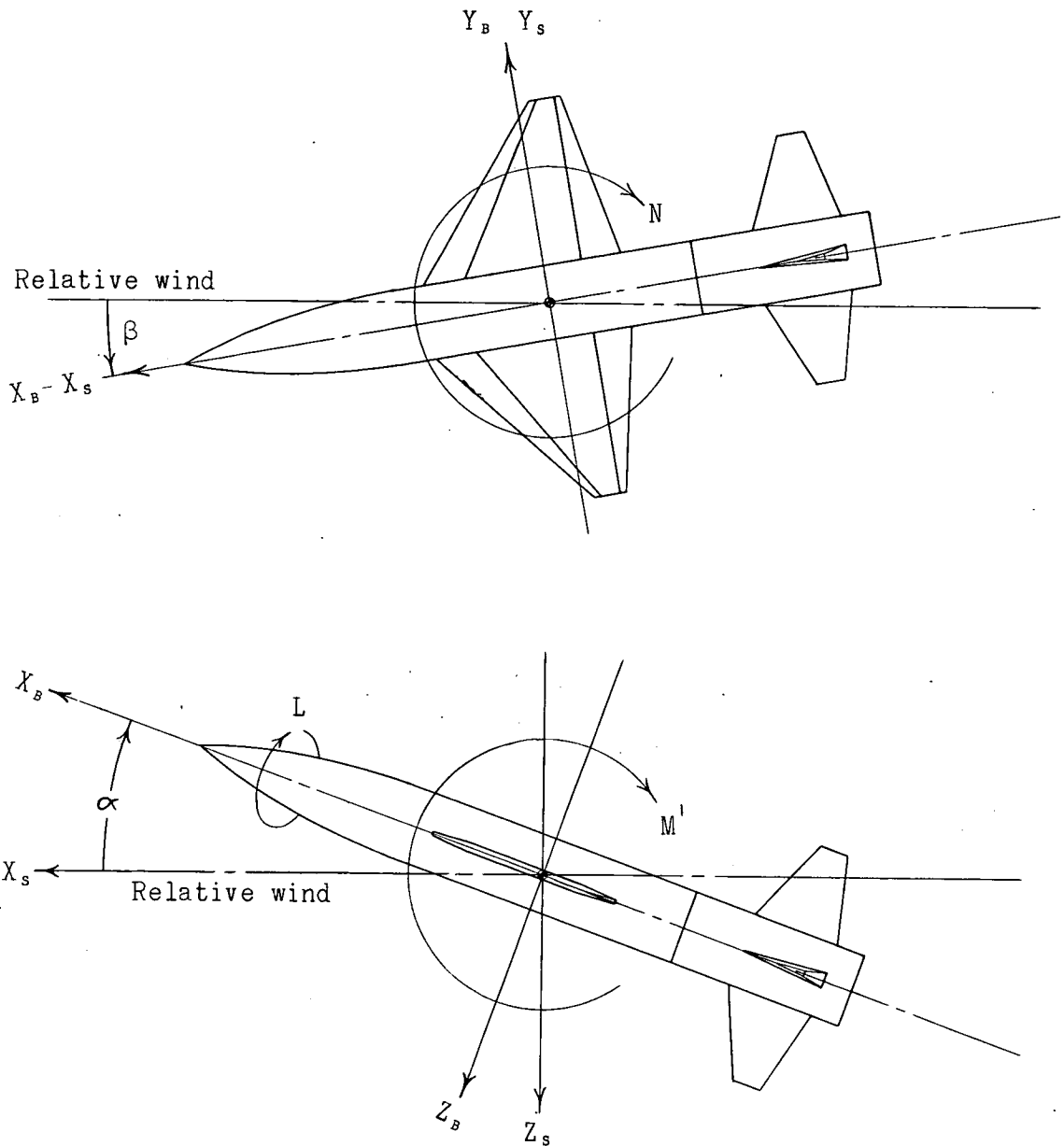


Figure 2.- Systems of reference axes.

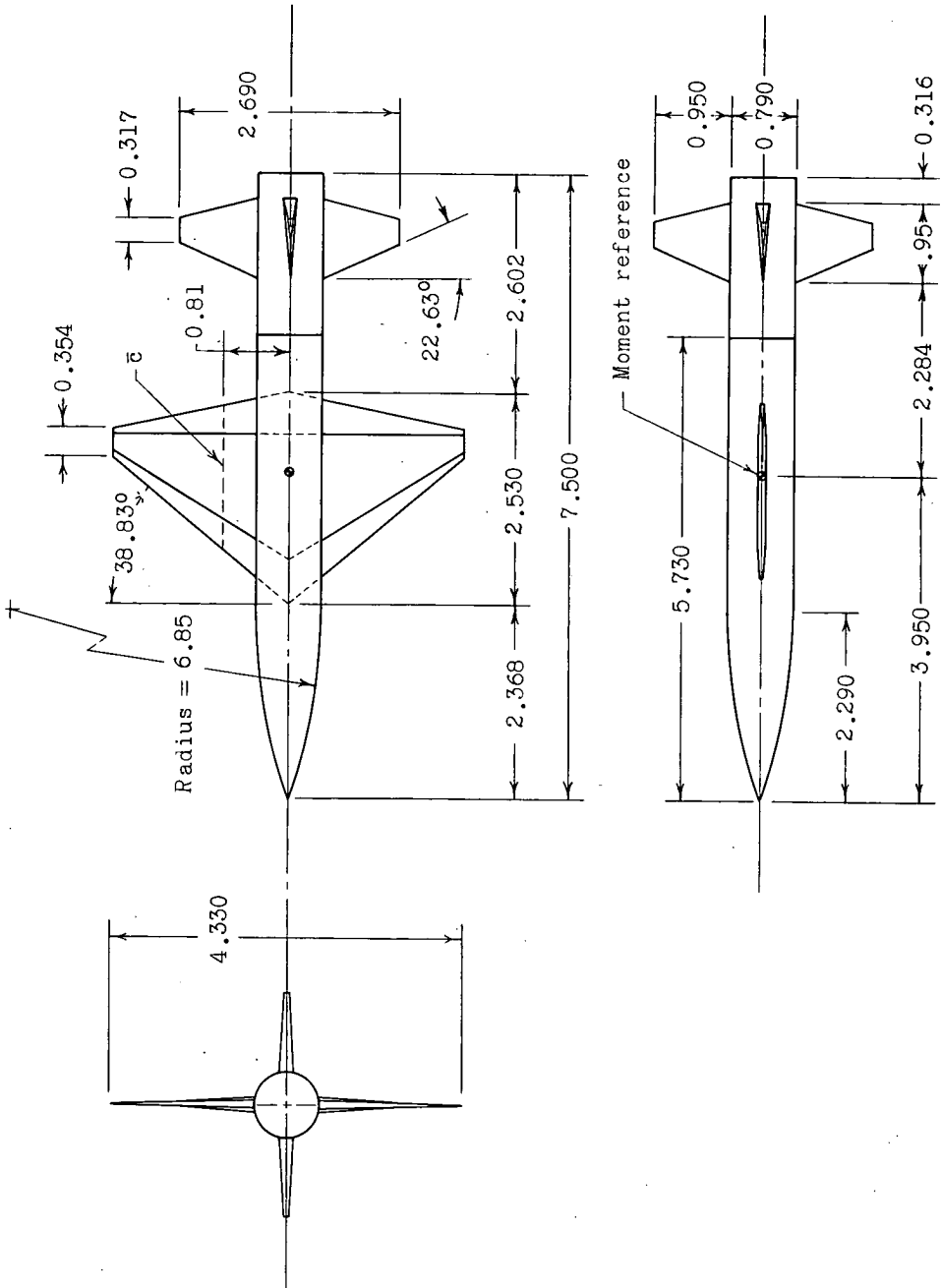
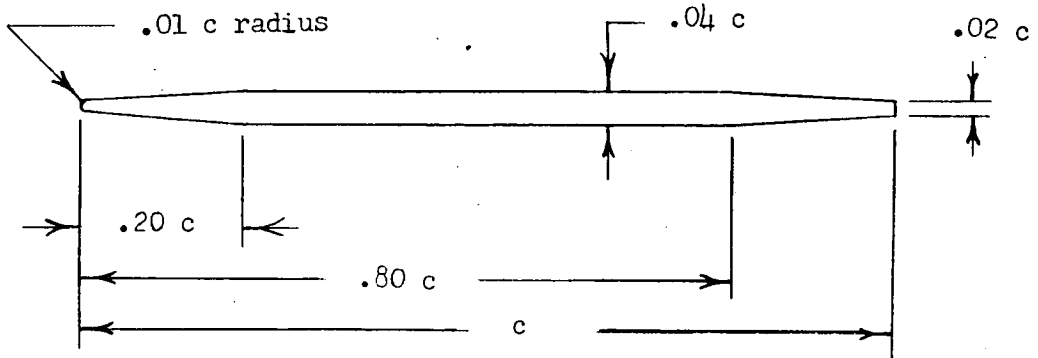
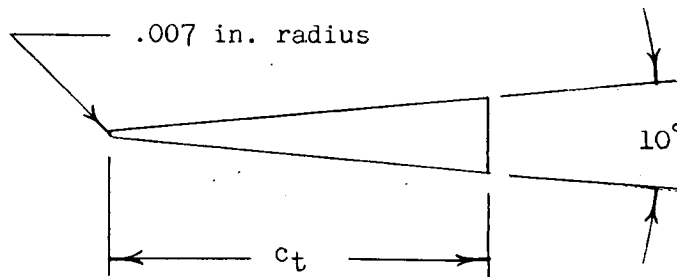


Figure 3.- Wind-tunnel model. All dimensions are in inches.

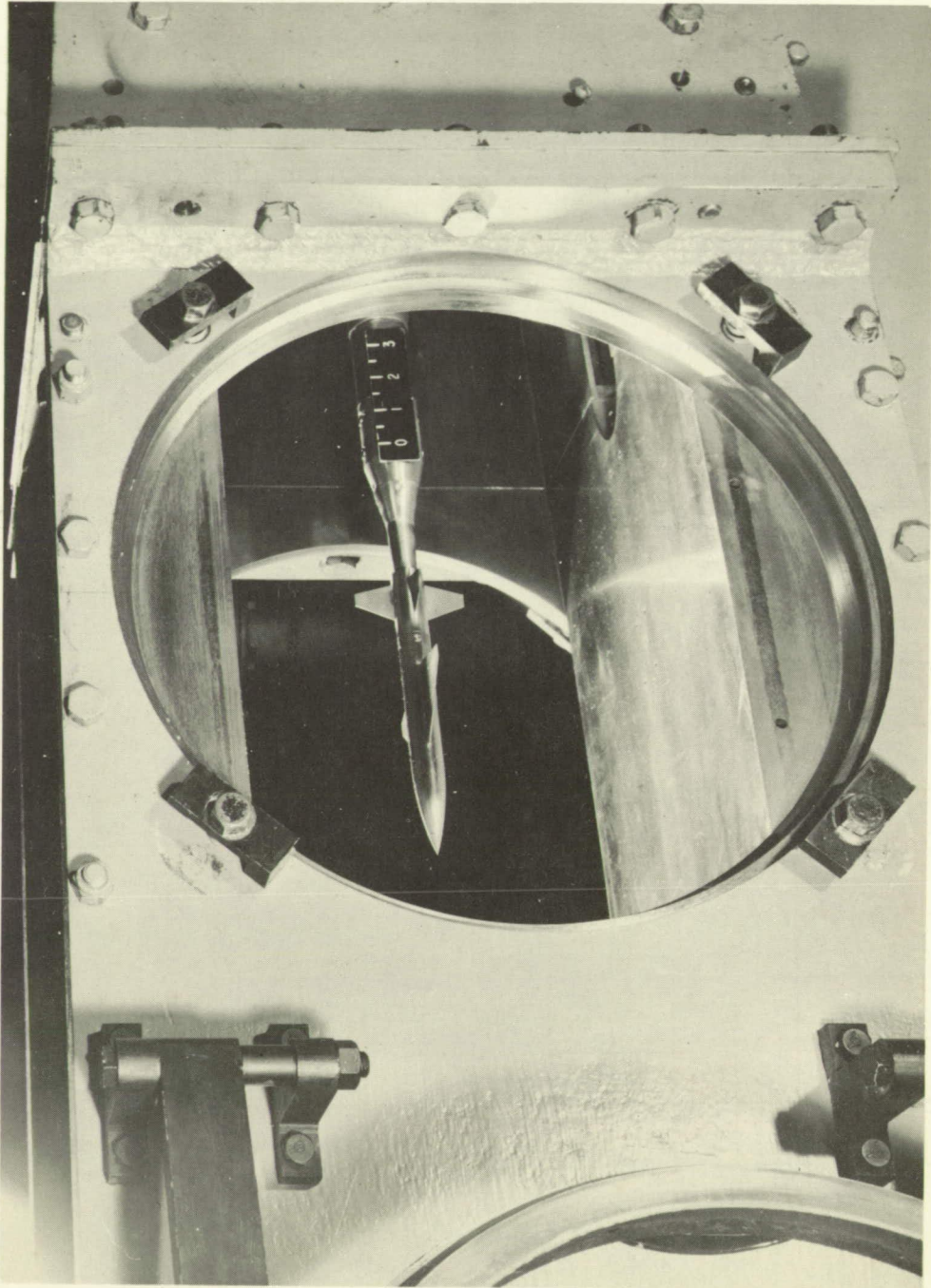


(a) Wing.



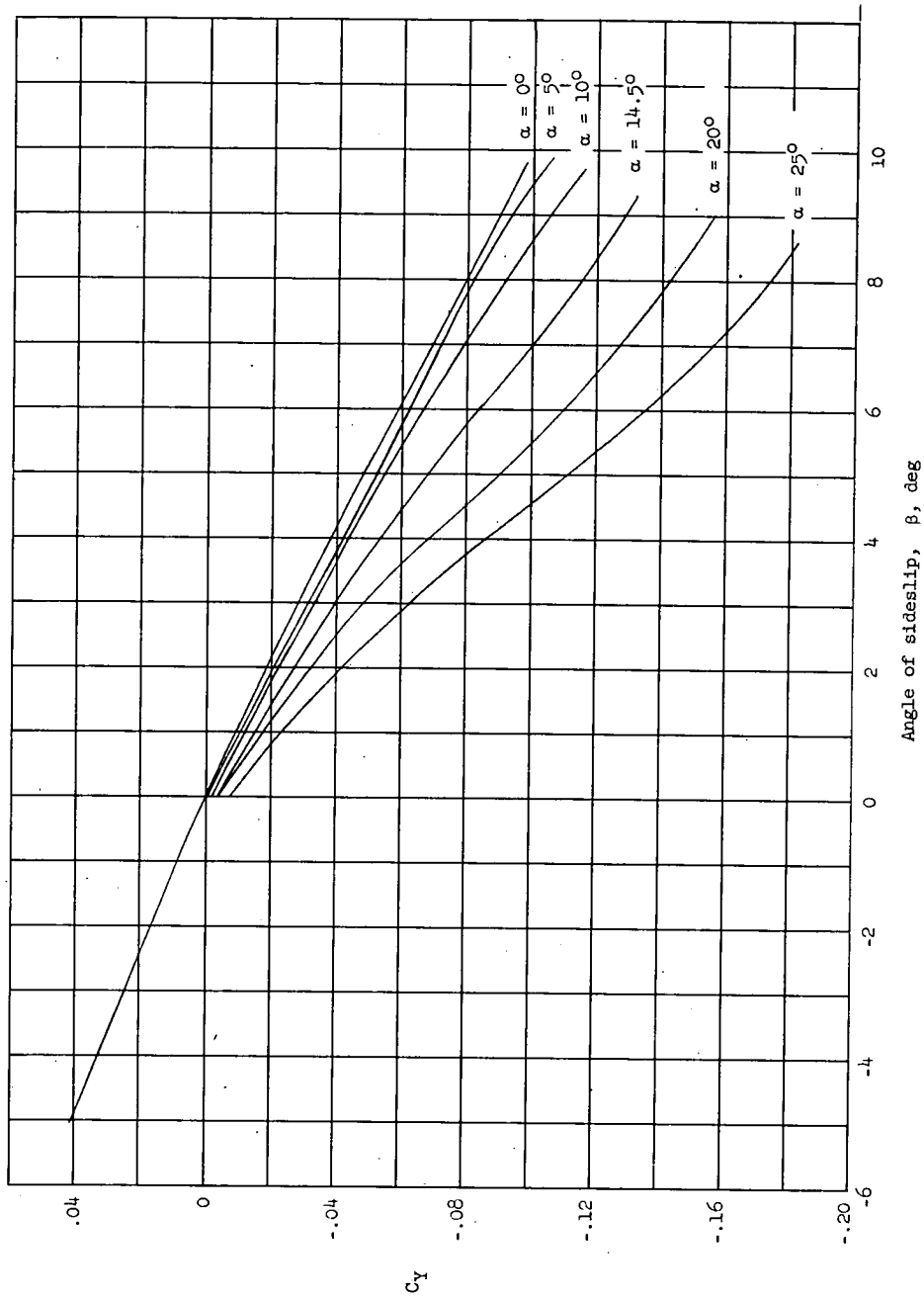
(b) Horizontal and vertical tails.

Figure 4.- Wing and tail airfoil sections used on model.



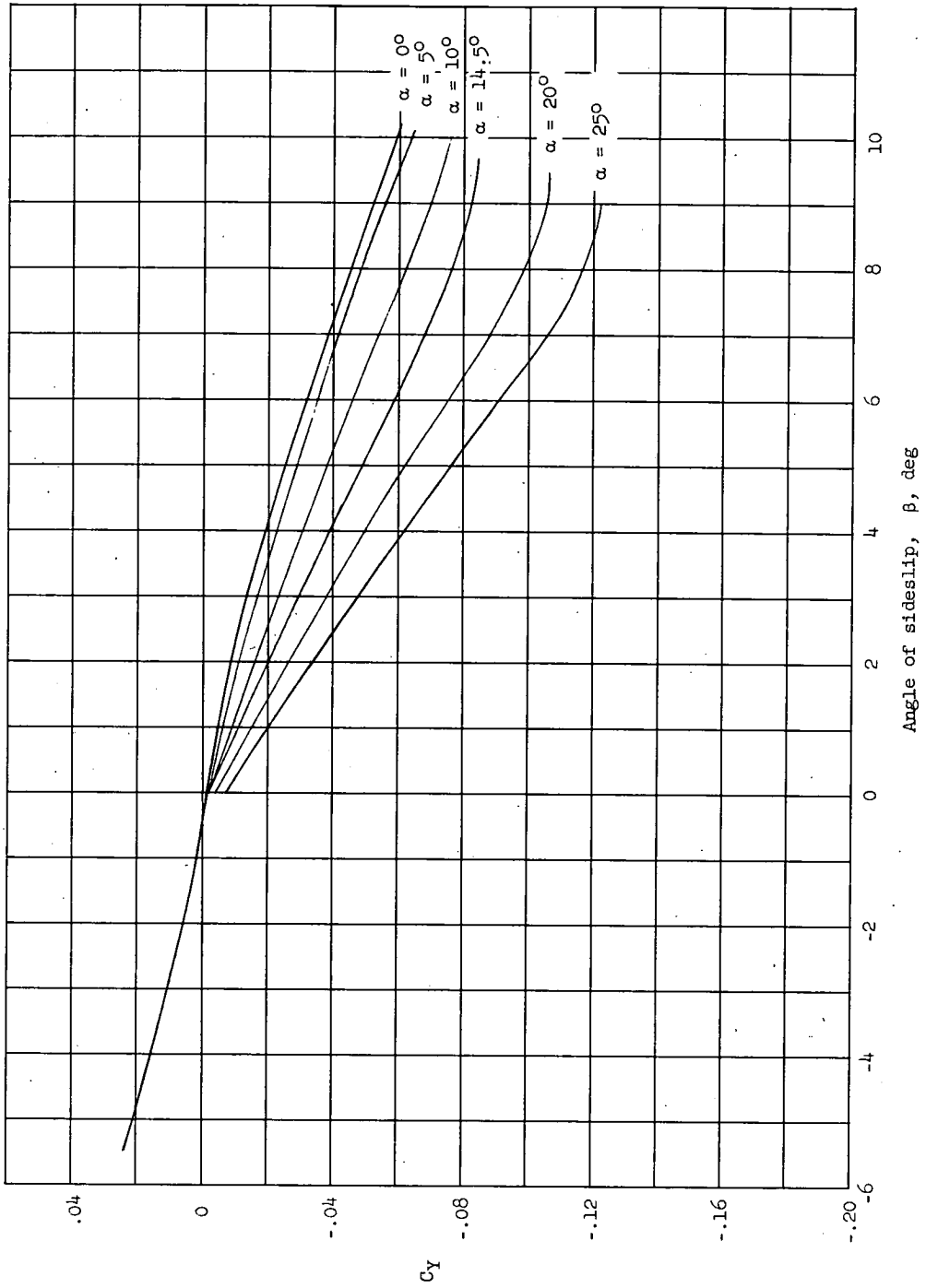
L-86712

Figure 5.- Installation of wind-tunnel model in the Langley 11-inch hypersonic tunnel.



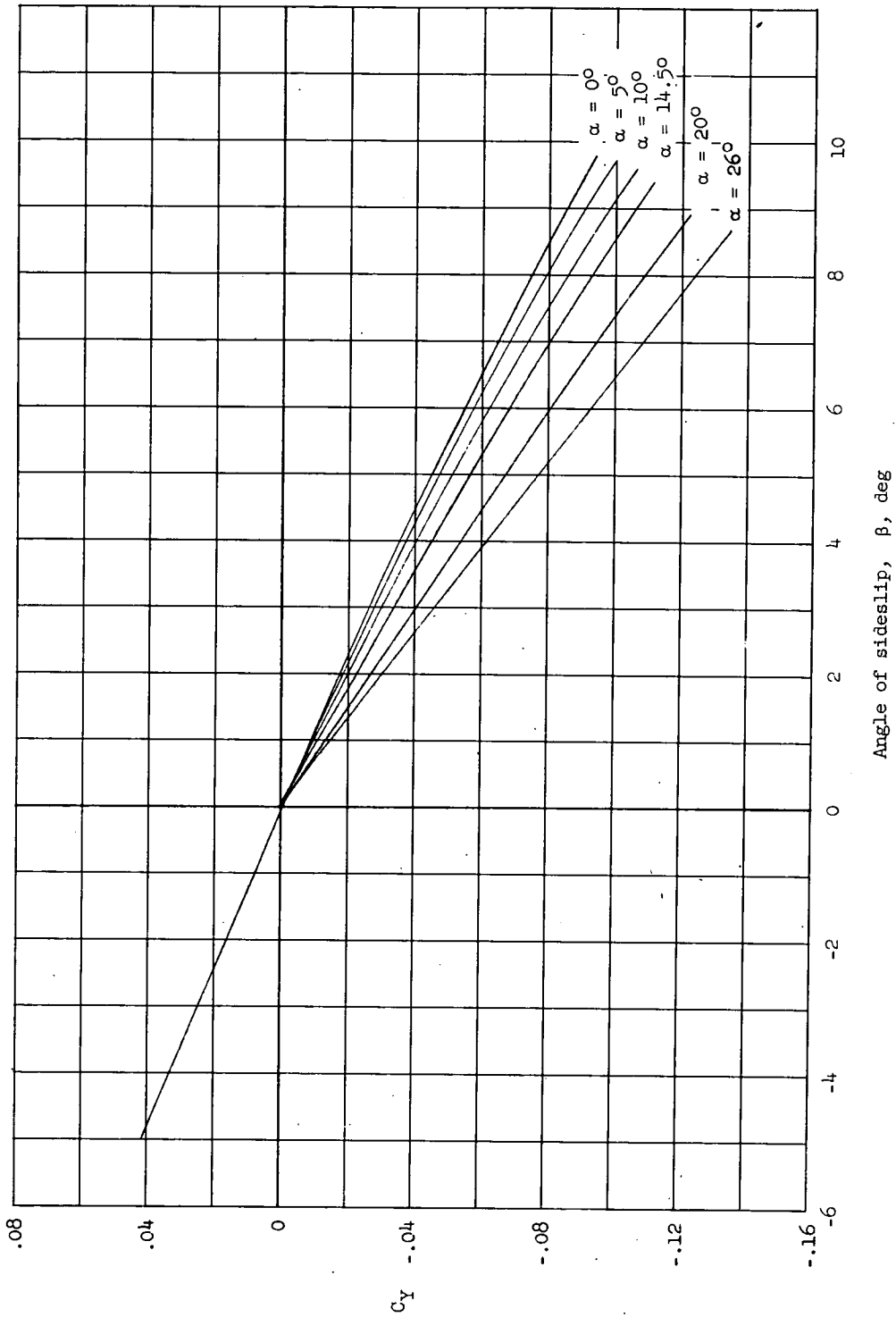
(a) Complete model.

Figure 6.- The variation of lateral-force coefficient with angle of sideslip for the model and its components. $M = 6.86$; $R = 343,000$; body-axis data.



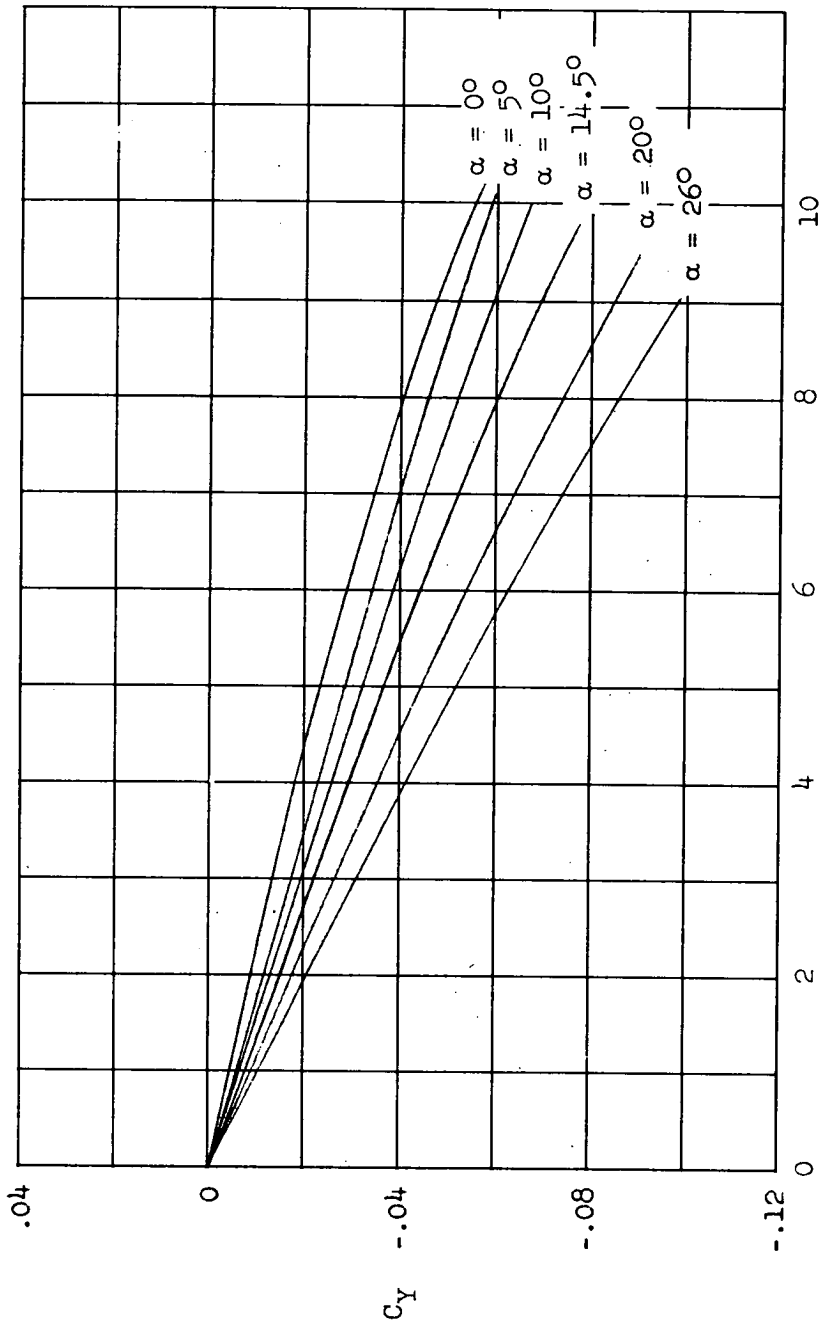
(b) Body-wing configuration.

Figure 6.- Continued.



(c) Body-tail configuration.

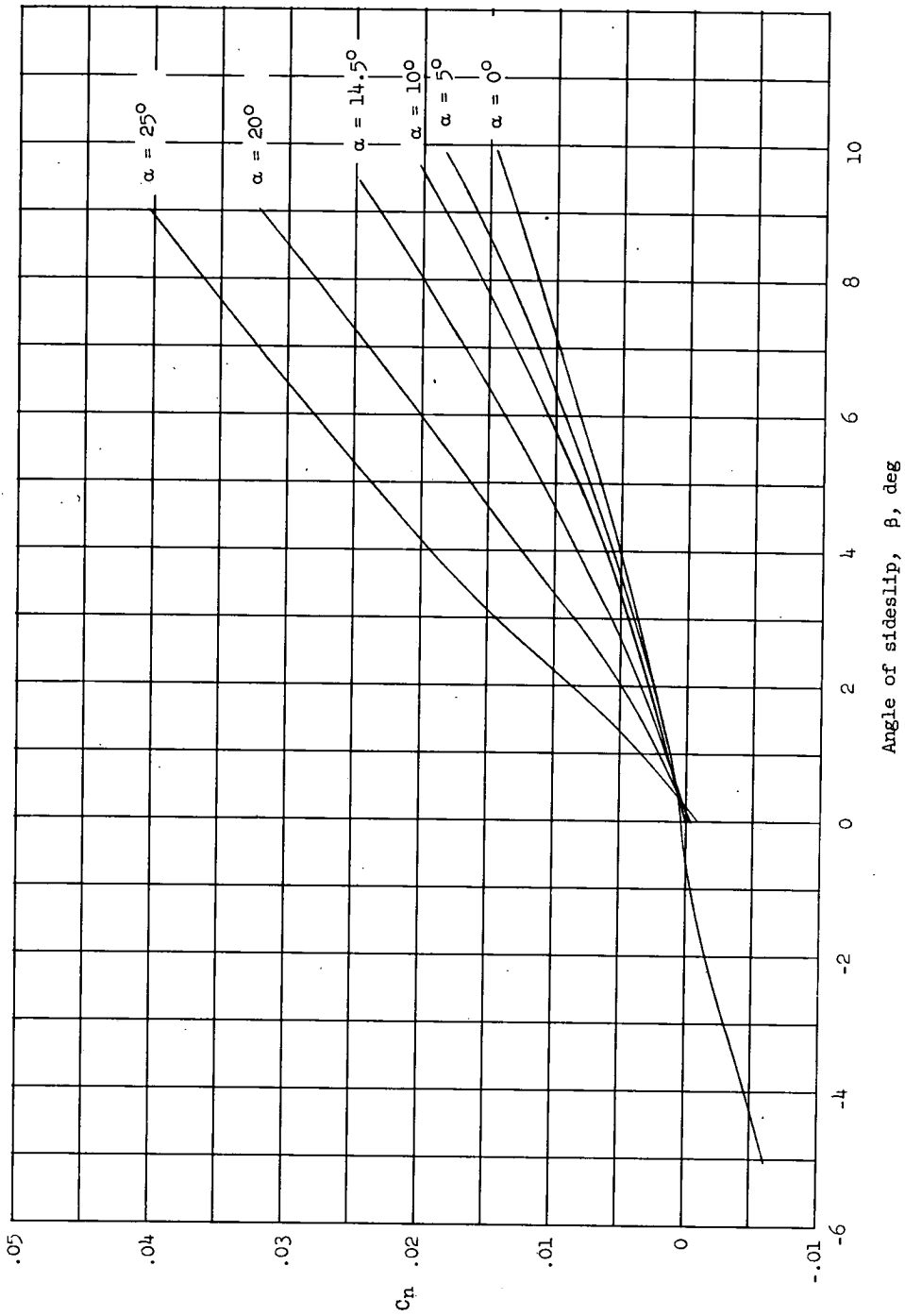
Figure 6.- Continued.



Angle of sideslip, β , deg

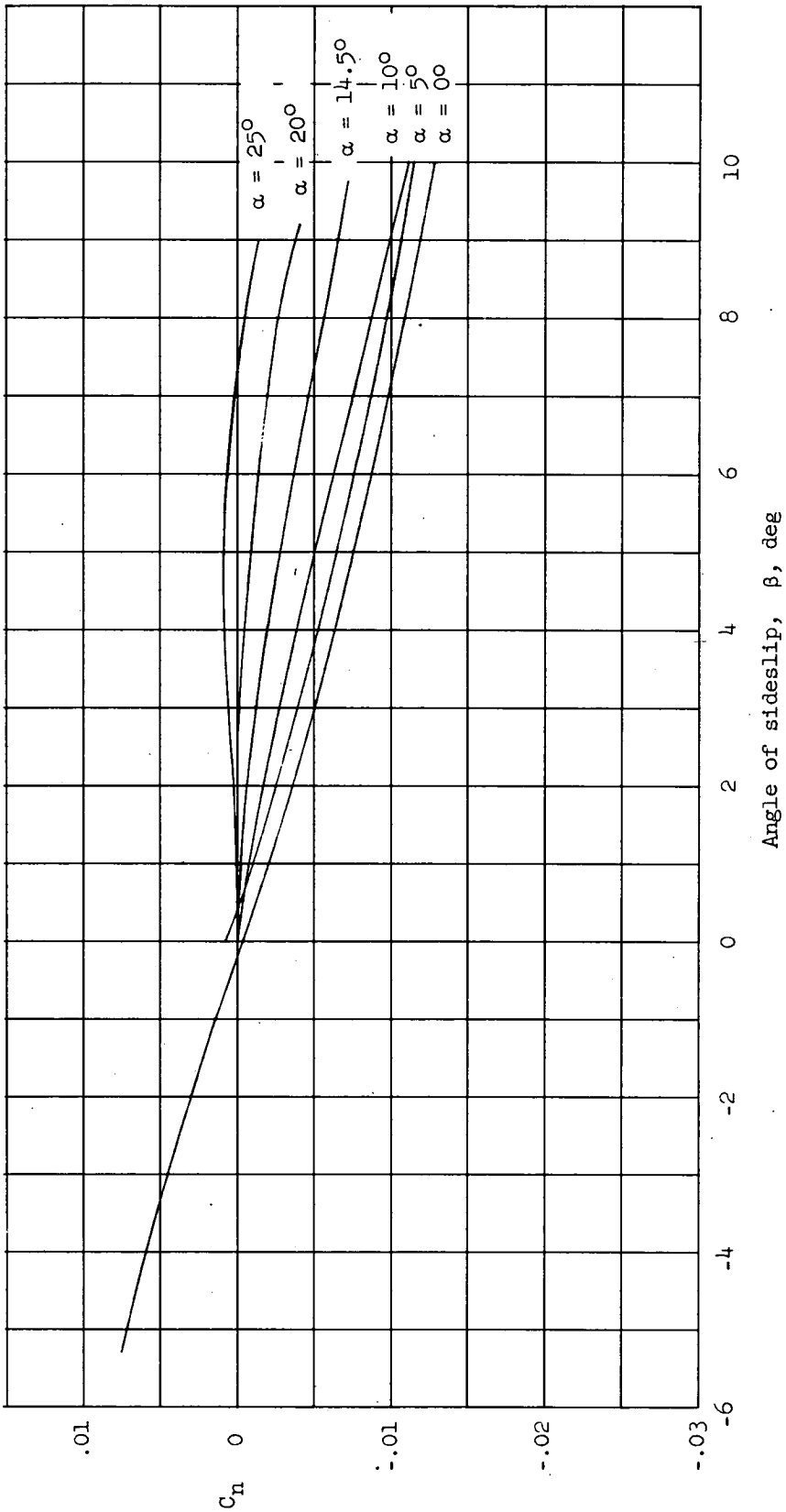
(d) Body-alone configuration.

Figure 6.- Concluded.



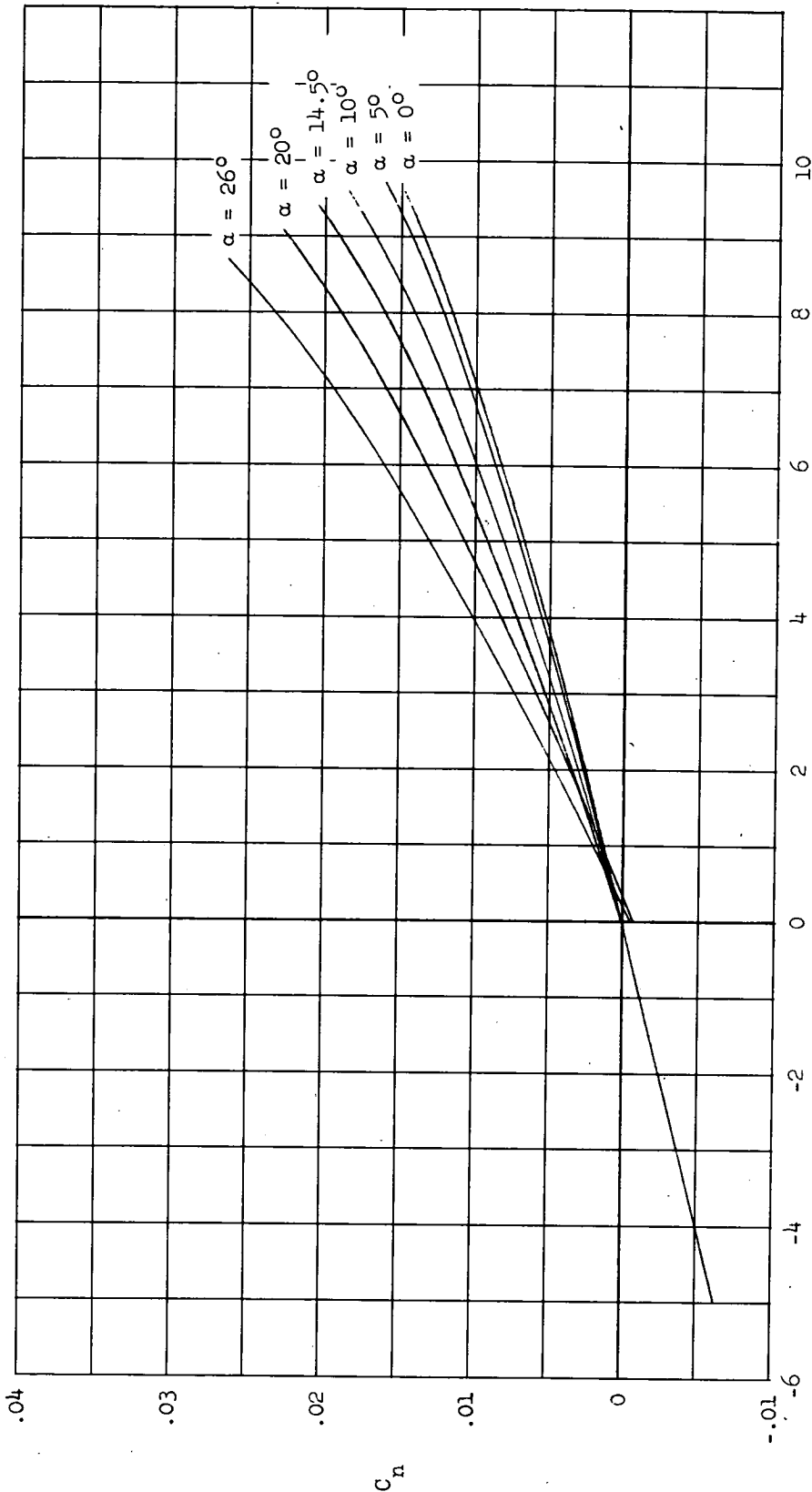
(a) Complete model.

Figure 7.- The variation of yawing-moment coefficient with angle of sideslip for the model and its components. $M = 6.86$; $R = 343,000$; body-axis data.



(b) Body-wing configuration.

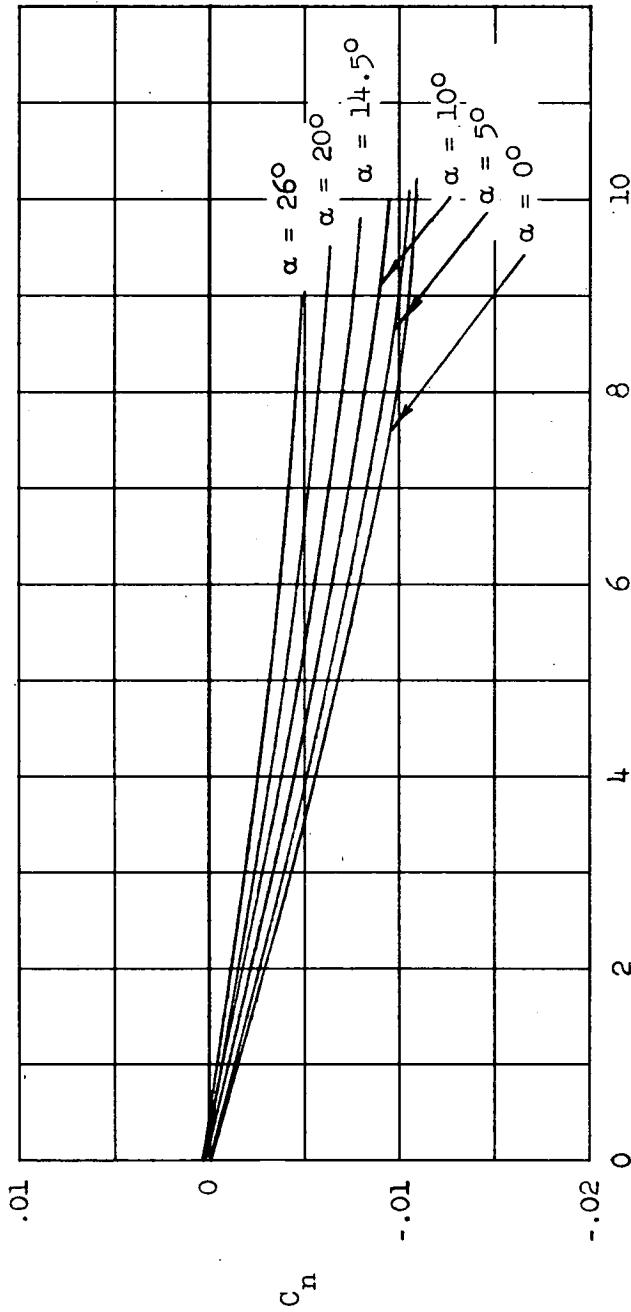
Figure 7.- Continued.



Angle of sideslip, β , deg

(c) Body-tail configuration.

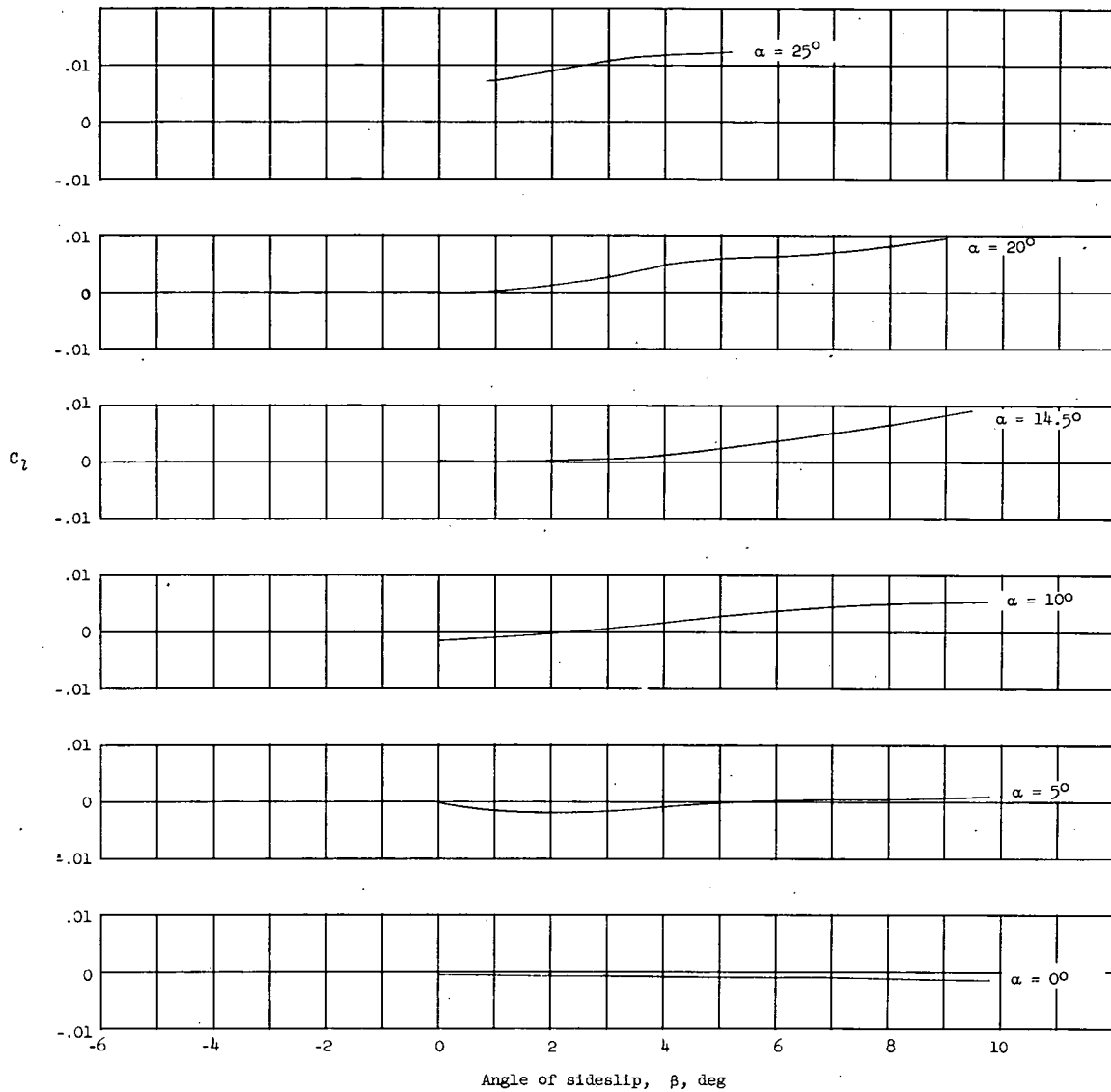
Figure 7.- Continued.



Angle of sideslip, β , deg

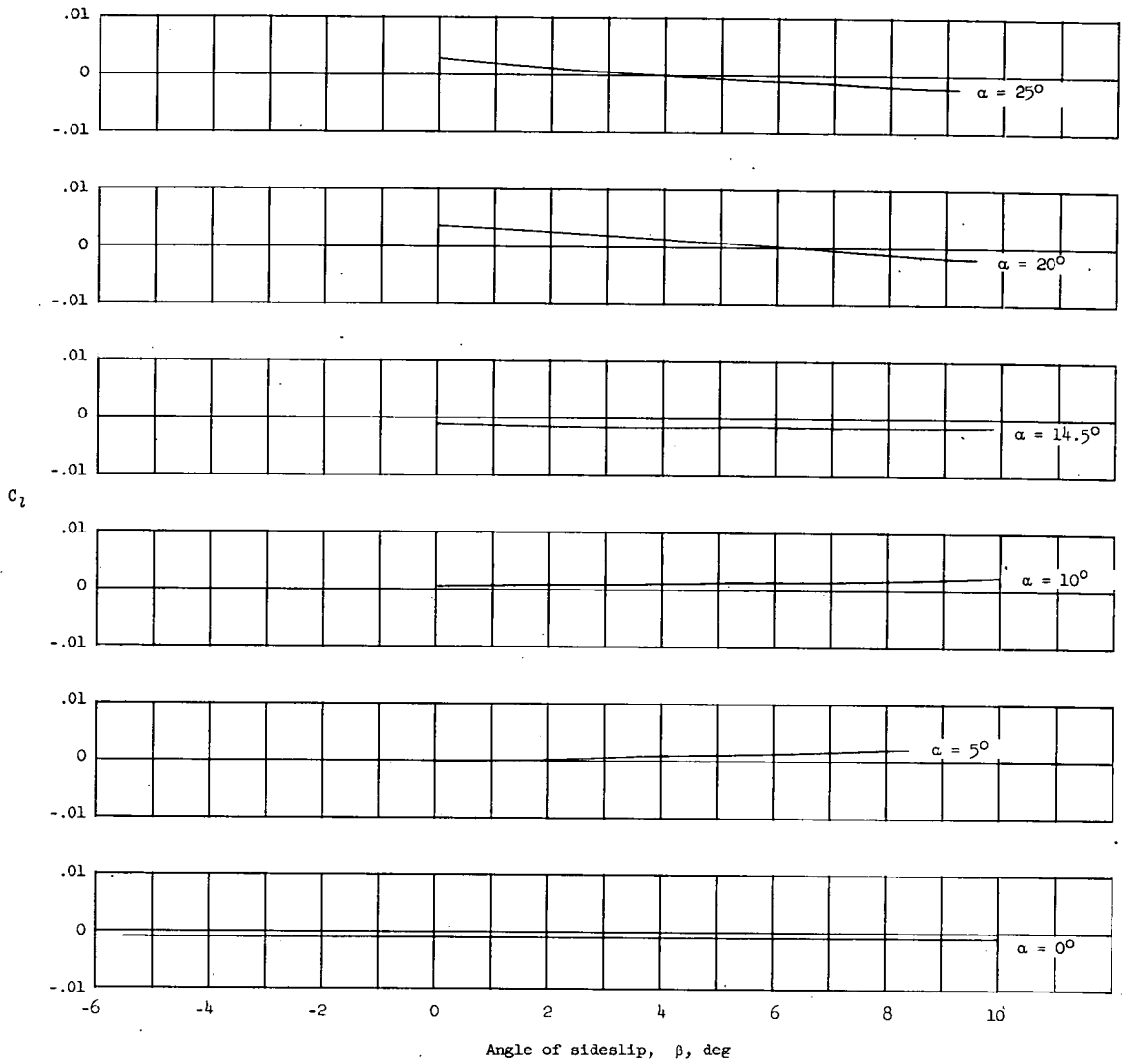
(d) Body-alone configuration.

Figure 7.- Concluded.



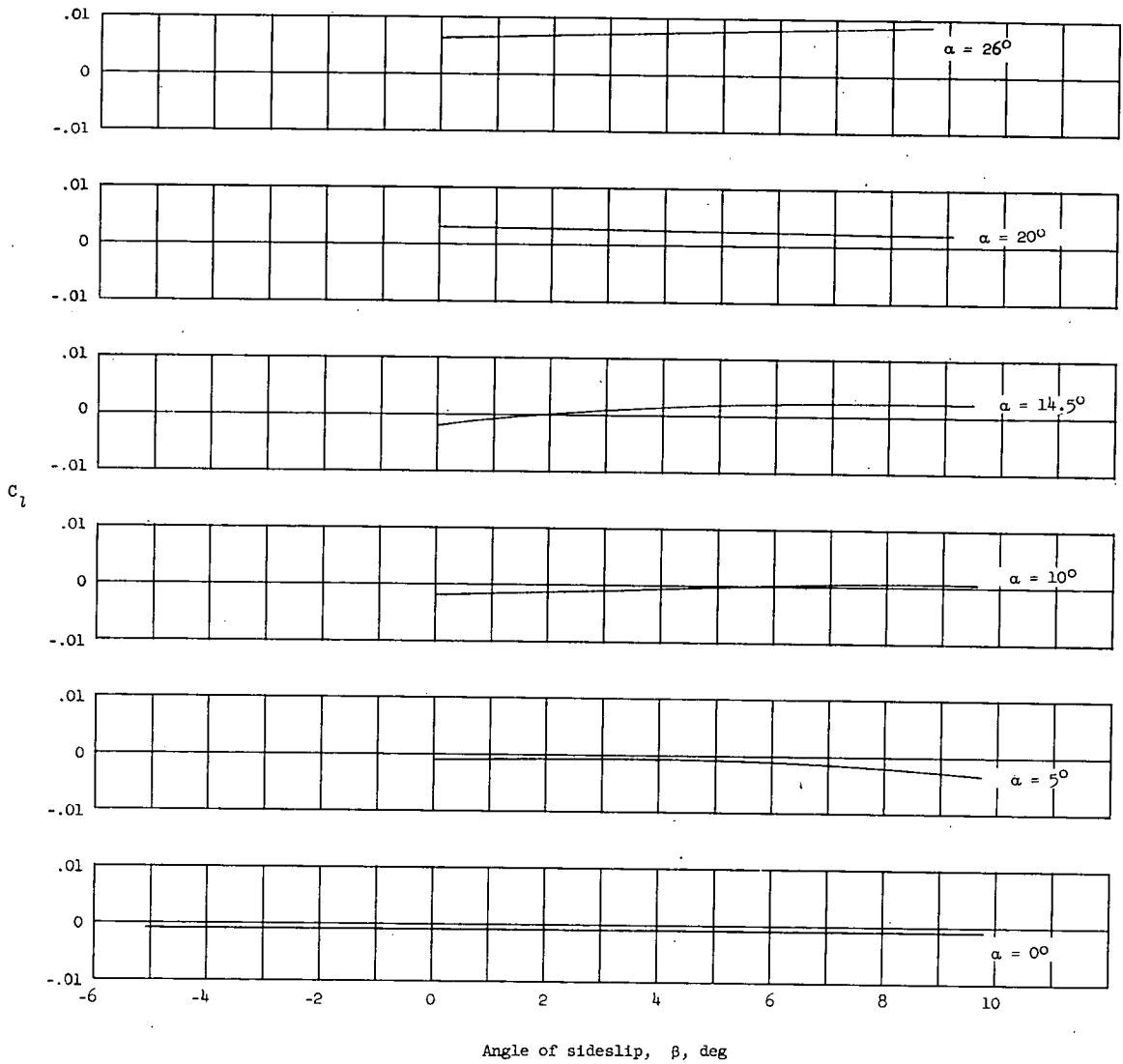
(a) Complete model.

Figure 8.- The variation of rolling-moment coefficient with angle of sideslip for the model and its components. $M = 6.86$; $R = 343,000$; body-axis data.



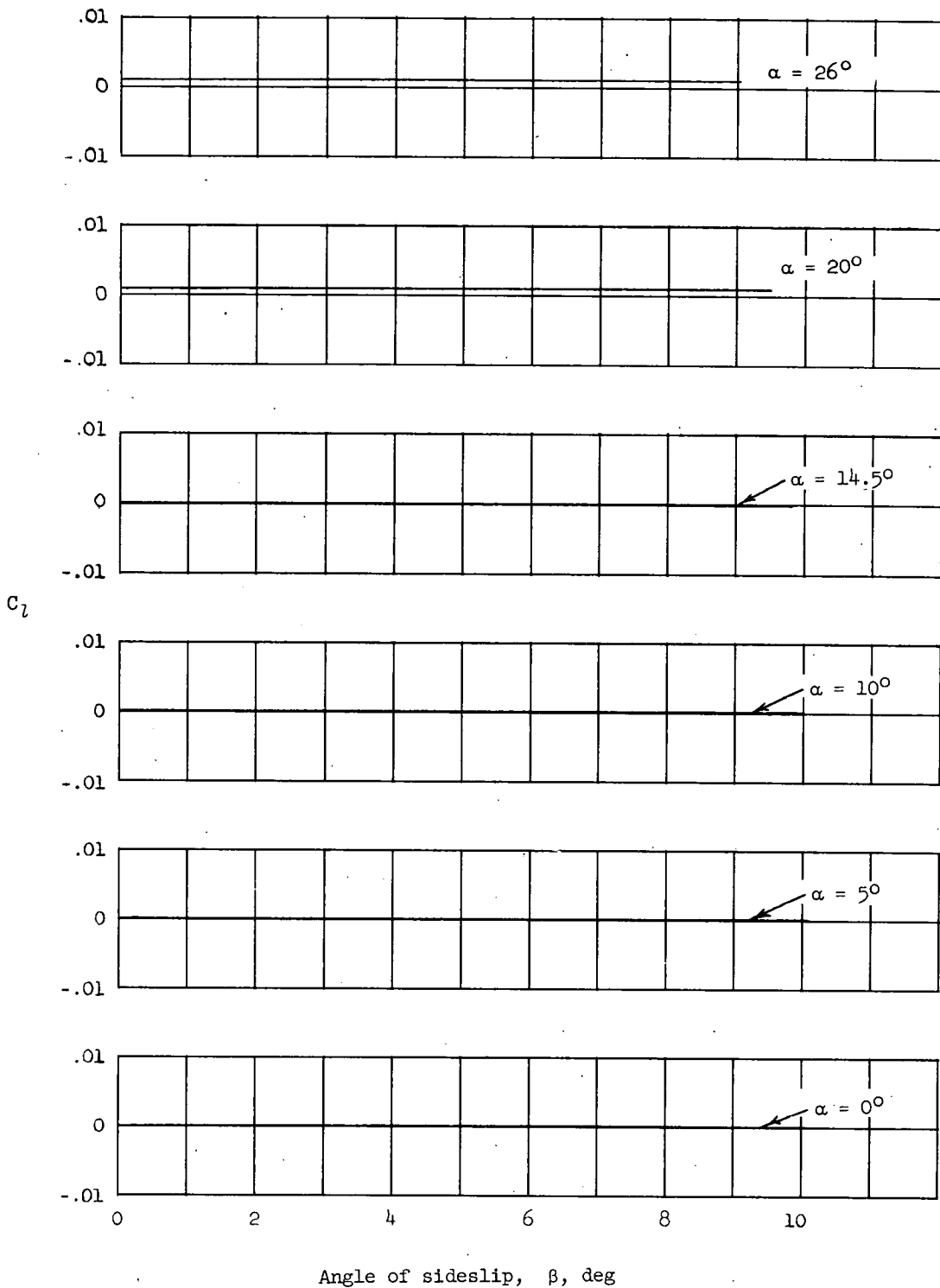
(b) Body-wing configuration.

Figure 8.- Continued.



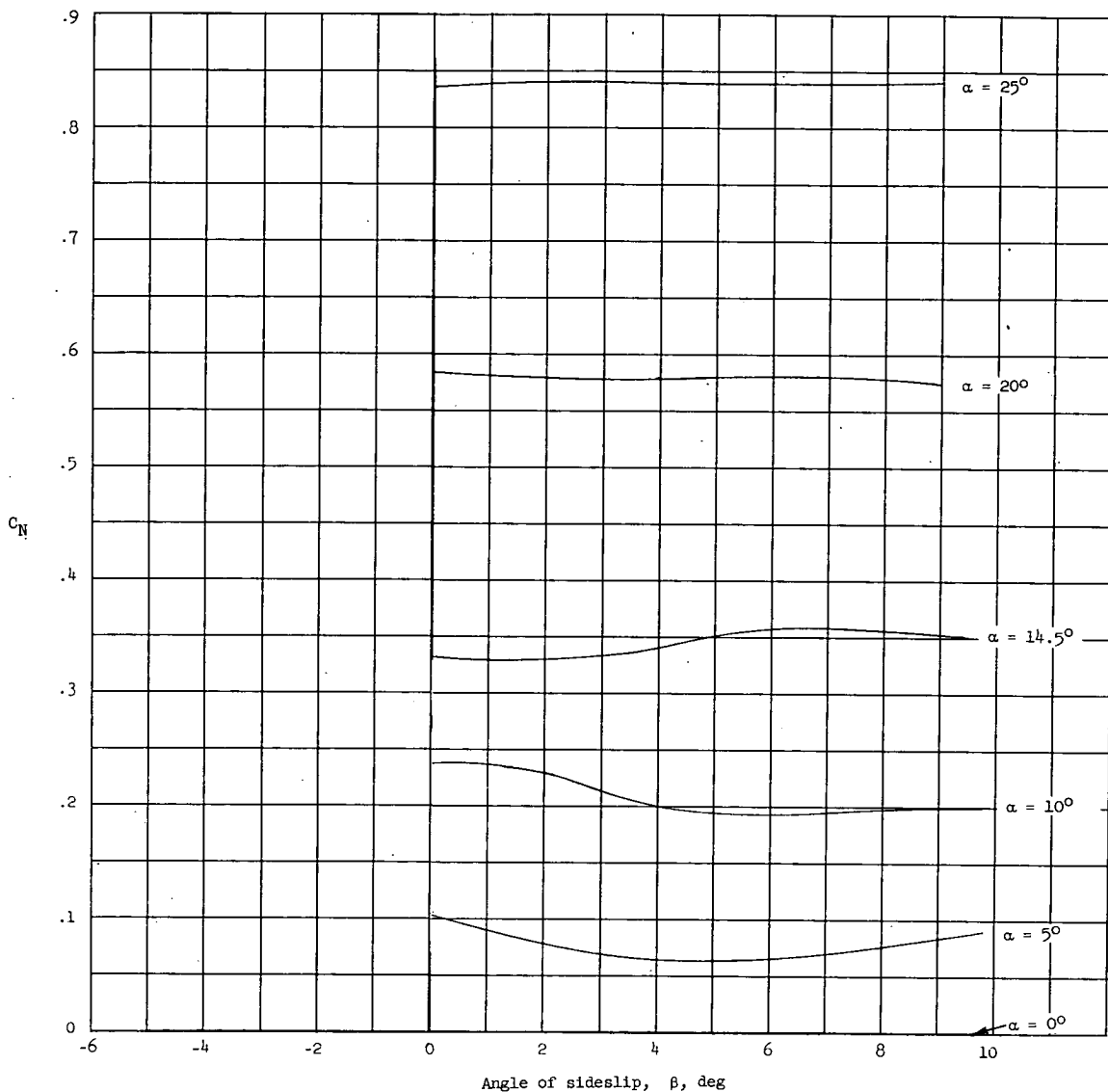
(c) Body-tail configuration.

Figure 8.- Continued.



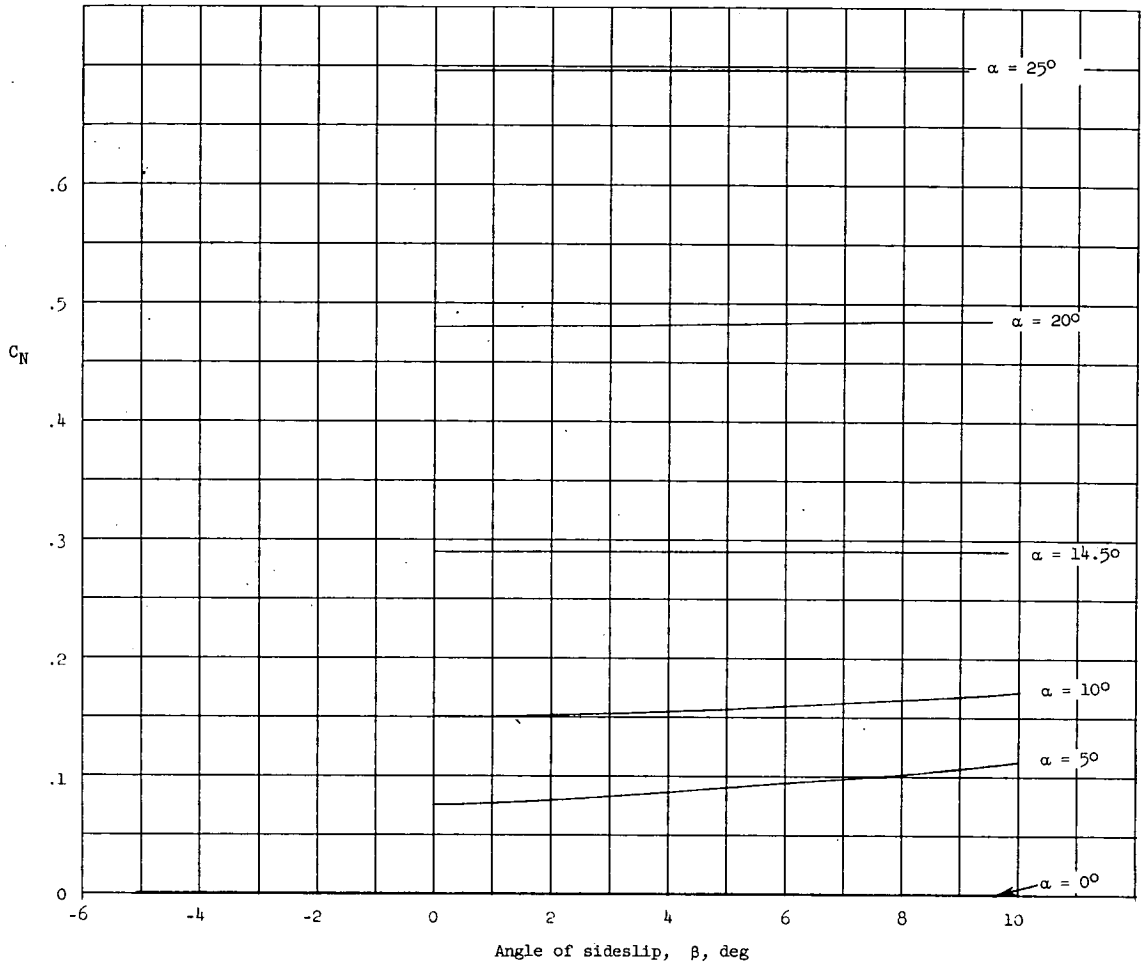
(d) Body-alone configuration.

Figure 8.- Concluded.



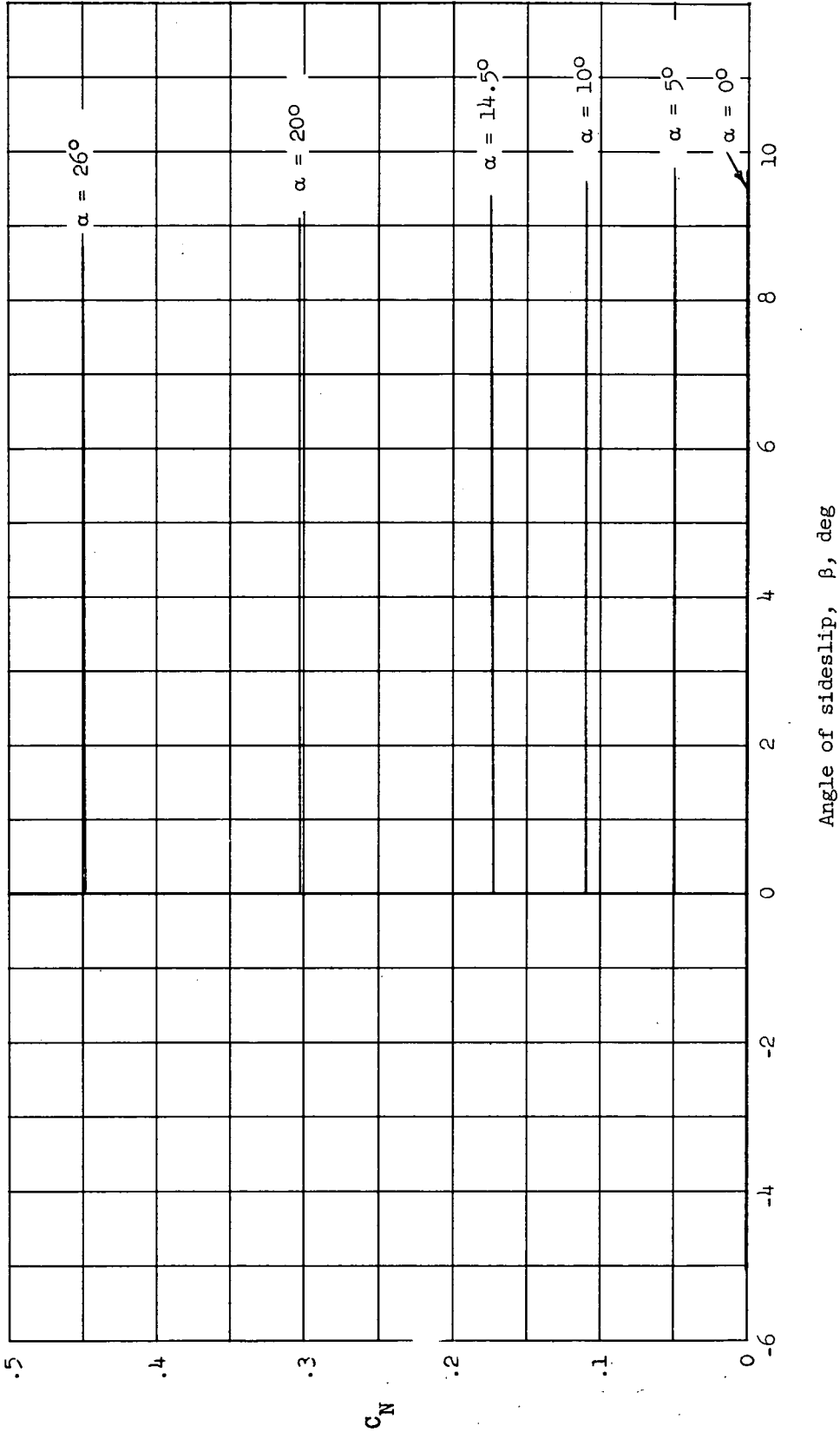
(a) Complete model.

Figure 9.- The variation of normal-force coefficient with angle of sideslip for the model and its components. $M = 6.86$; $R = 343,000$; body-axis data.



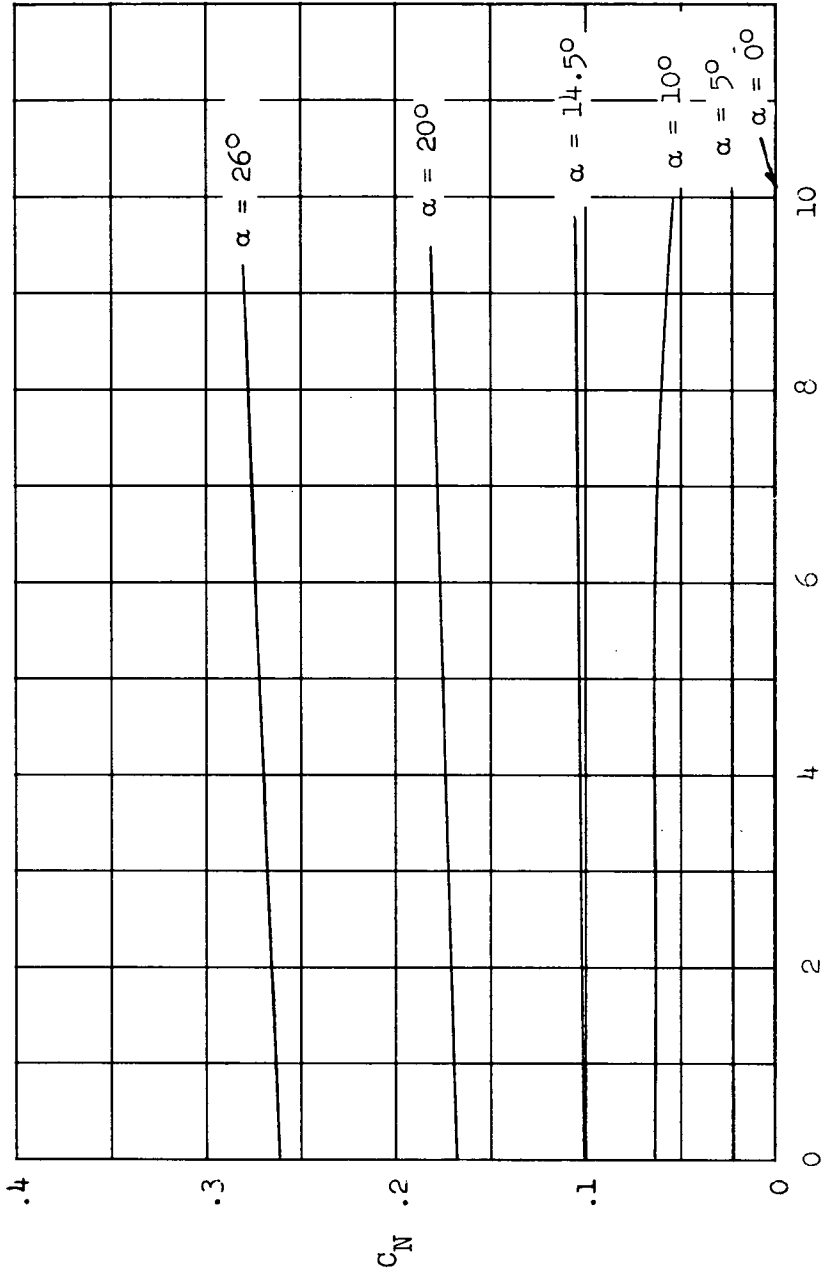
(b) Body-wing configuration.

Figure 9.- Continued.



(c) Body-tail configuration.

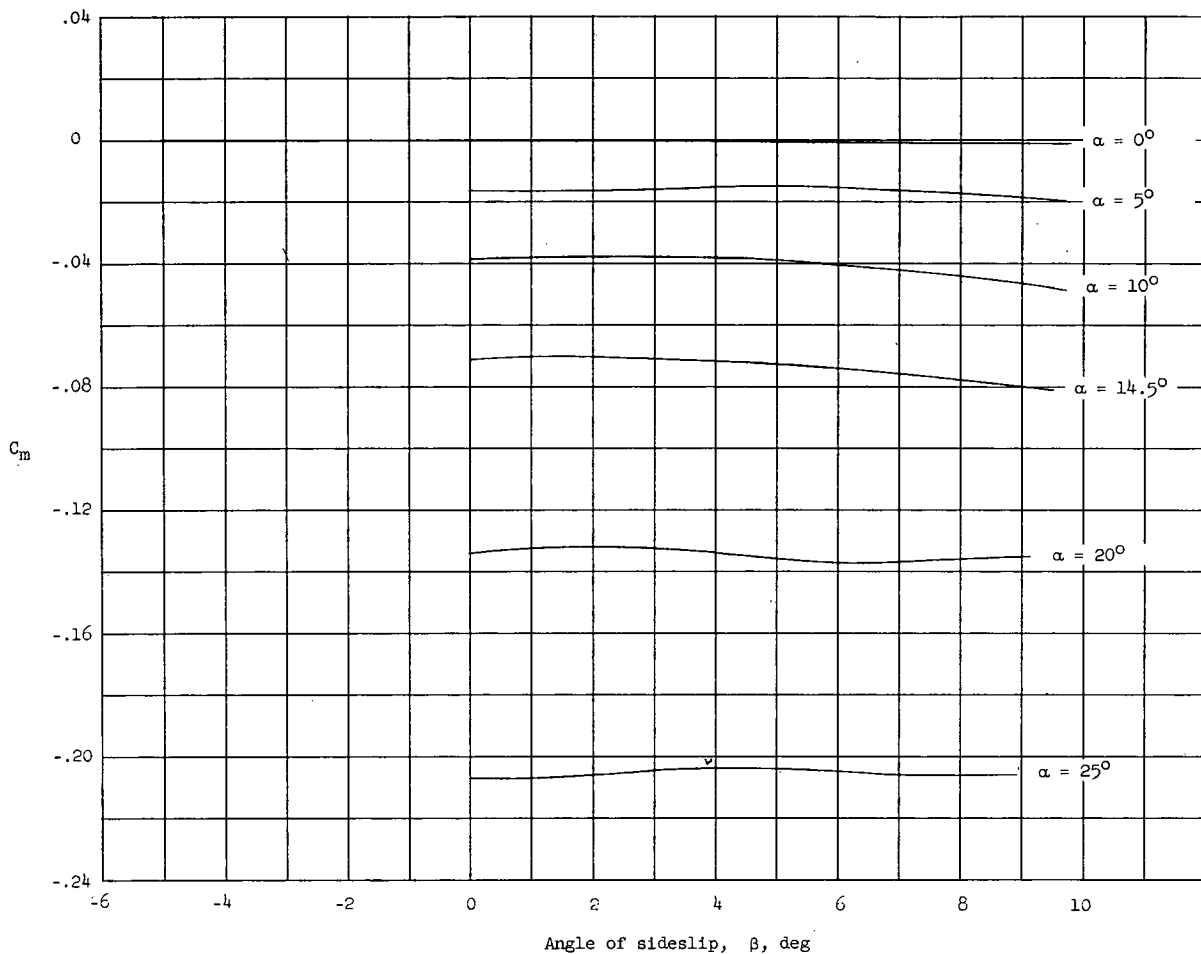
Figure 9.- Continued.



Angle of sideslip, β , deg

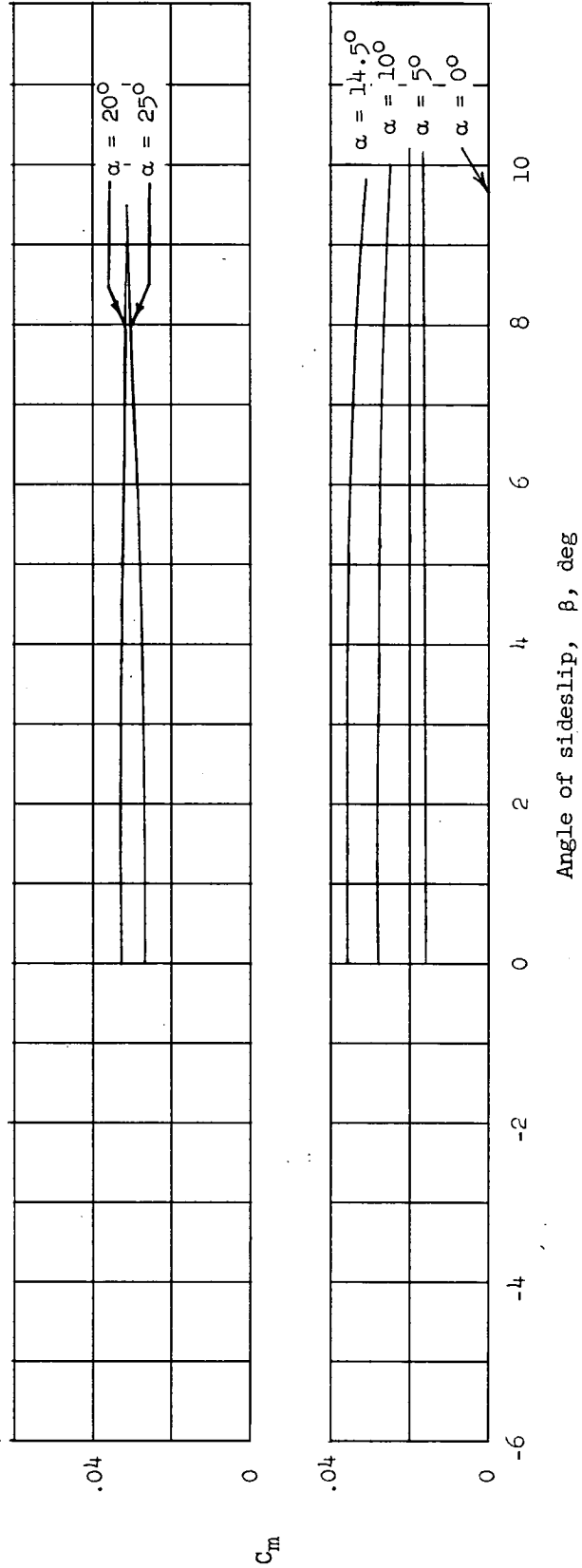
(d) Body-alone configuration.

Figure 9.- Concluded.



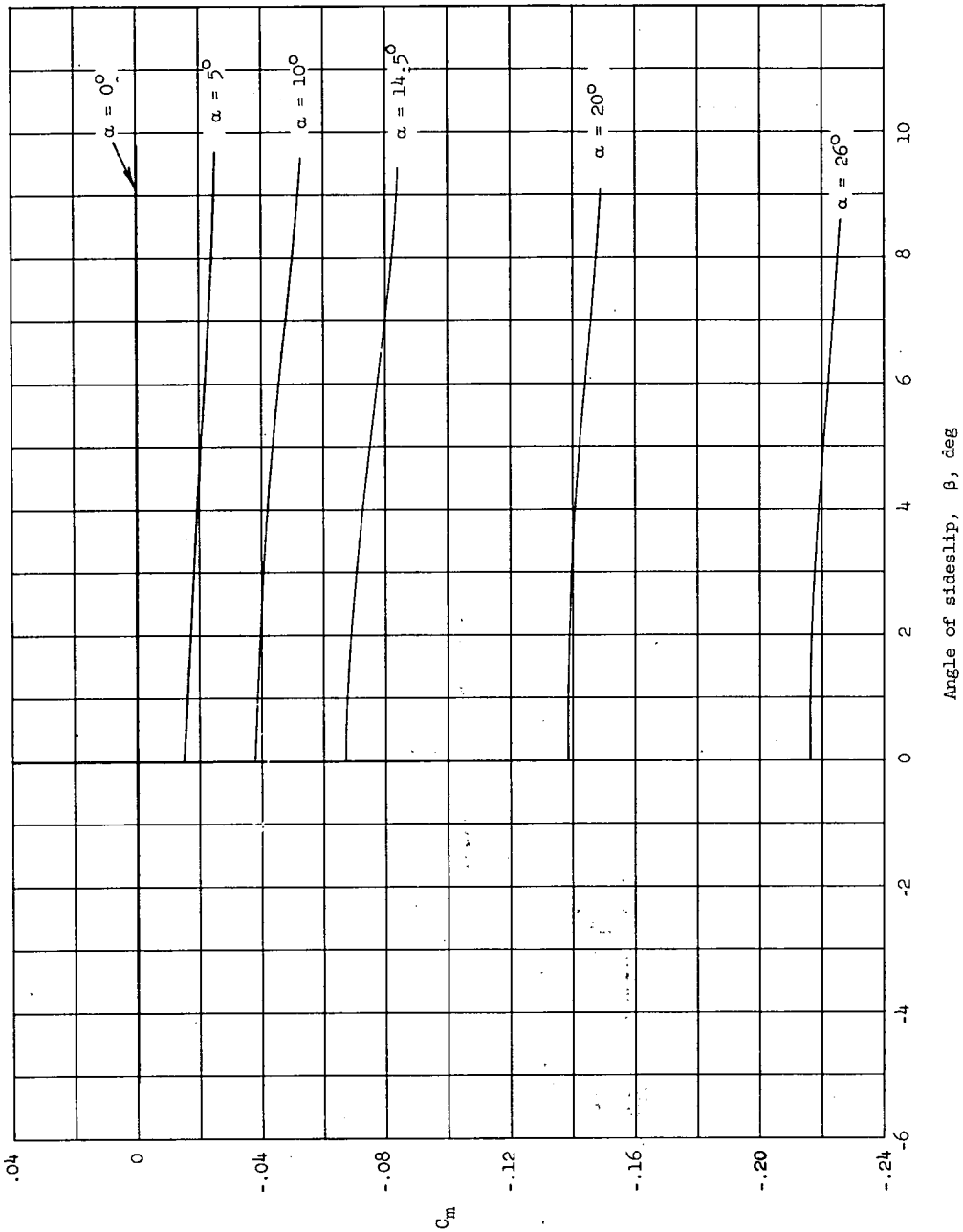
(a) Complete model.

Figure 10.- The variation of pitching-moment coefficient with angle of sideslip for the model and its components. $M = 6.86$; $R = 343,000$; body-axis data.



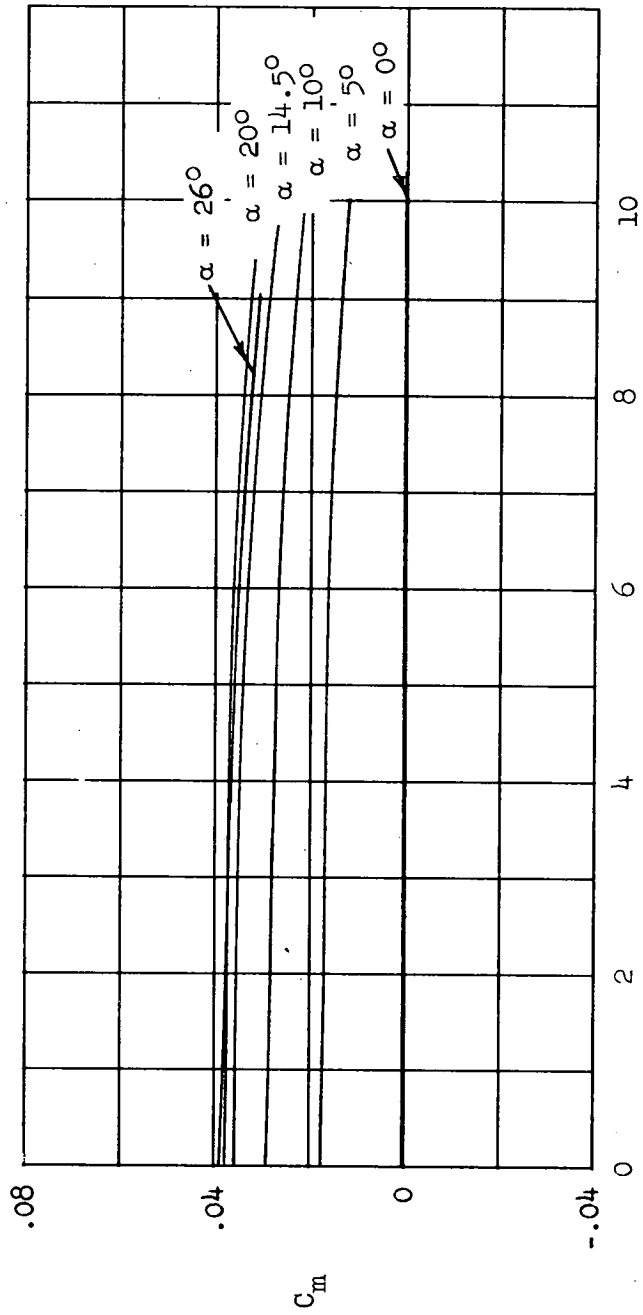
(b) Body-wing configuration.

Figure 10.- Continued.



(c) Body-tail configuration.

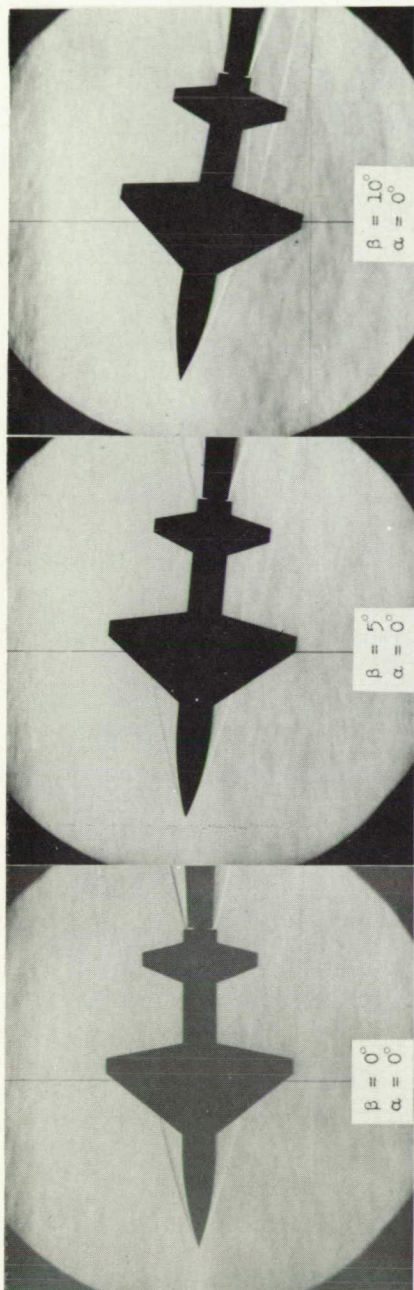
Figure 10.- Continued.



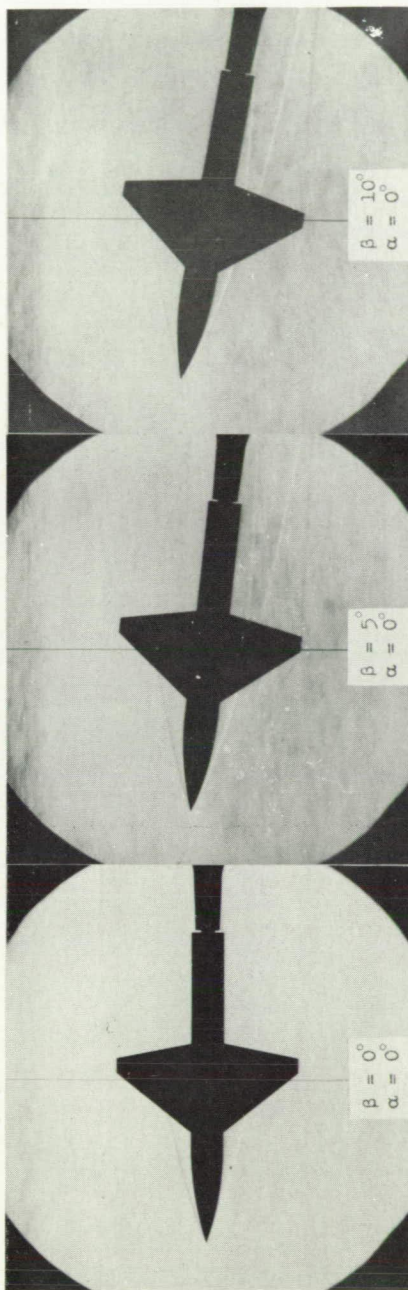
Angle of sideslip, β , deg

(d) Body-alone configuration.

Figure 10.- Concluded.



(a) Complete model.



(b) Body-wing configuration. L-87525

Figure 11.-- Typical schlieren photographs of complete-model and the body-wing configuration. $M = 6.86$; $R = 343,000$.

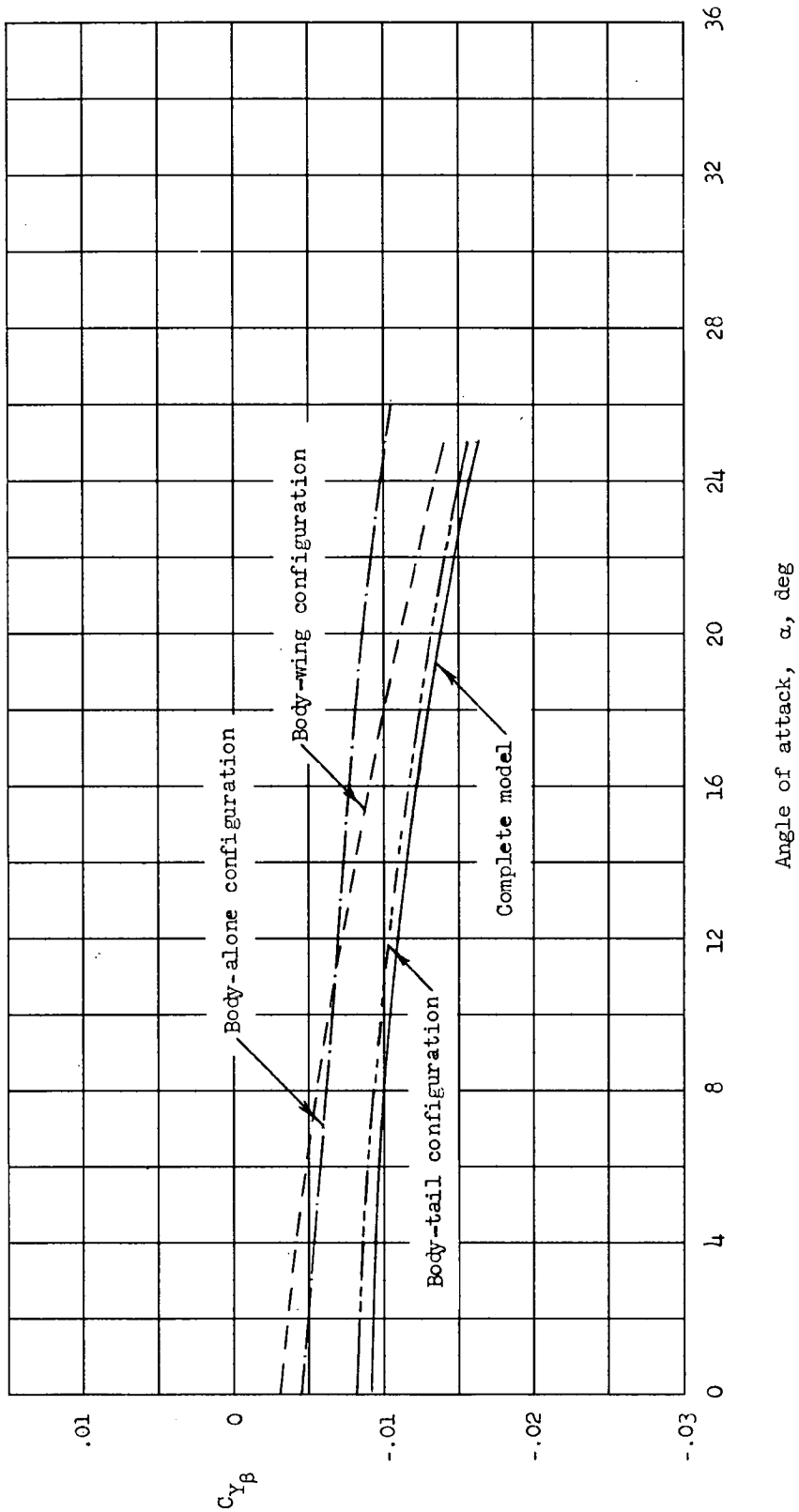


Figure 12.- The variation of $C_{Y_{\beta}}$ with angle of attack for the complete model and its components. $M = 6.86$; $R = 343,000$; body-axis data.

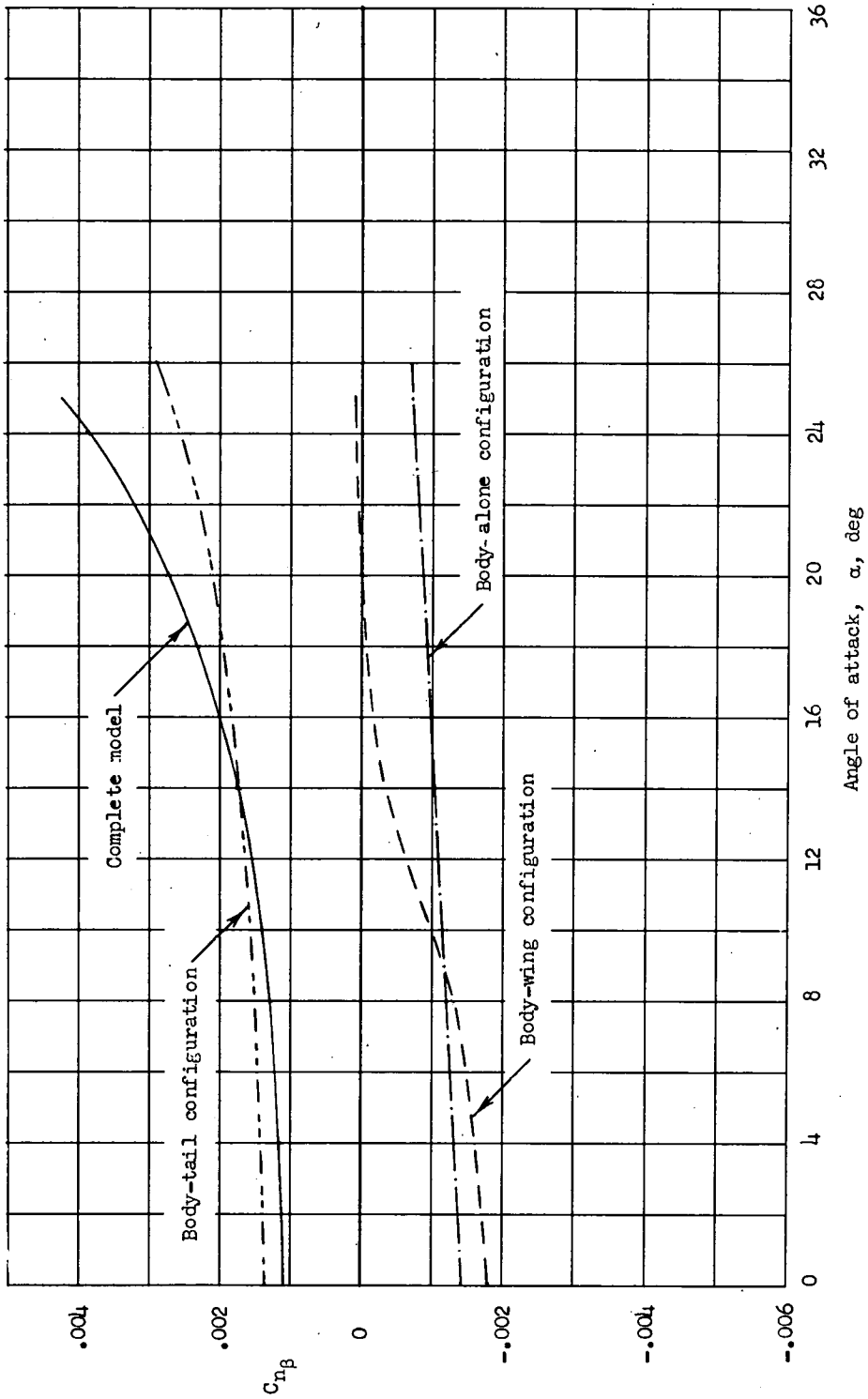


Figure 13.- The variation of $C_{n\beta}$ with angle of attack for the complete model and its components. $M = 6.86$; $R = 343,000$; body-axis data.

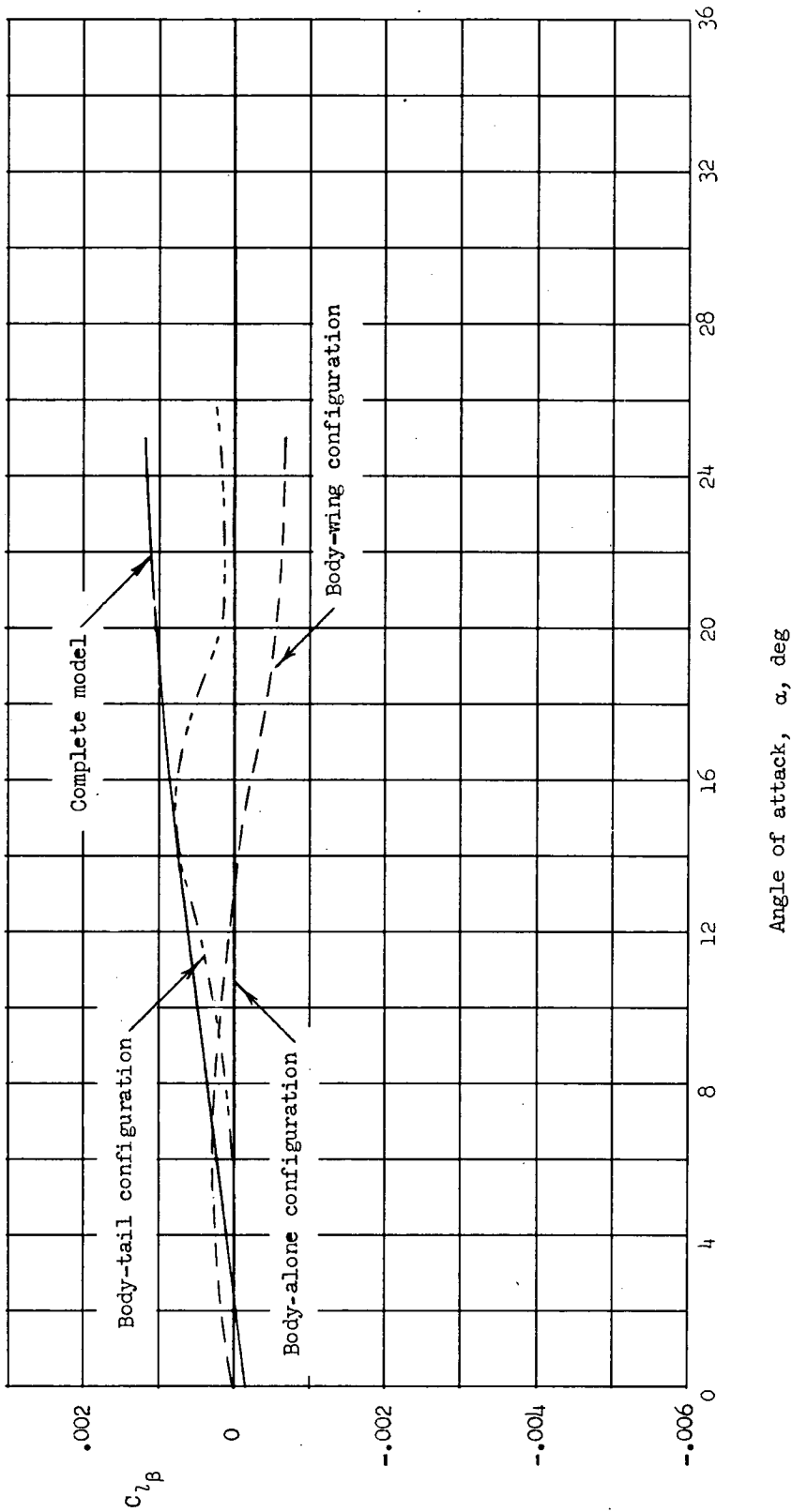


Figure 14.- The variation of $C_{l\beta}$ with angle of attack for the complete model and its components. $M = 6.86$; $R = 343,000$; body-axis data.

